nature geoscience

ARTICLES

https://doi.org/10.1038/s41561-022-00925-2

Check for updates

Substantial carbon drawdown potential from enhanced rock weathering in the United Kingdom

Euripides P. Kantzas[1], Maria Val Martin[1], Mark R. Lomas[1], Rafael M. Eufrasio[2], Phil Renforth[3], Amy L. Lewis[1], Lyla L. Taylor[1], Jean-Francois Mecure[4,5], Hector Pollitt[5,6], Pim V. Vercoulen[4,6], Negar Vakilifard[7], Philip B. Holden[7], Neil R. Edwards[5,7], Lenny Koh[2], Nick F. Pidgeon[8], Steven A. Banwart[9,10] and David J. Beerling[1]✉

Achieving national targets for net-zero carbon emissions will require atmospheric carbon dioxide removal strategies compatible with rising agricultural production. One possible method for delivering on these goals is enhanced rock weathering, which involves modifying soils with crushed silicate rocks, such as basalt. Here we use dynamic carbon budget modelling to assess the carbon dioxide removal potential and agricultural benefits of implementing enhanced rock weathering strategies across UK arable croplands. We find that enhanced rock weathering could deliver net carbon dioxide removal of 6–30 $MtCO_2\,yr^{-1}$ for the United Kingdom by 2050, representing up to 45% of the atmospheric carbon removal required nationally to meet net-zero emissions. This suggests that enhanced rock weathering could play a crucial role in national climate mitigation strategies if it were to gain acceptance across national political, local community and farm scales. We show that it is feasible to eliminate the energy-demanding requirement for milling rocks to fine particle sizes. Co-benefits of enhanced rock weathering include substantial mitigation of nitrous oxide, the third most important greenhouse gas, widespread reversal of soil acidification and considerable cost savings from reduced fertilizer usage. Our analyses provide a guide for other nations to pursue their carbon dioxide removal ambitions and decarbonize agriculture—a key source of greenhouse gases.

Governments worldwide are increasingly translating the Paris Agreement under the United Nations Framework Convention on Climate Change into national strategies for achieving net-zero carbon emissions by 2050. More than 120 nations have set full decarbonization goals that account for 51% of global CO_2 emissions, with the United Kingdom among several of these nations legislating for net-zero emissions[1]. The United Kingdom, where the industrial revolution driven by burning fossil fuels originated, is responsible for ~5% of the cumulative CO_2 emissions over the period 1751–2018 that drive climate change[2]. Carbon emissions in the United Kingdom have declined by 43% between 1990 and 2018 owing to the rise of renewables, and the transition from coal to natural gas, while growing the economy by 75% (ref. [3]). Continued phase-out of emissions is, however, required to meet the United Kingdom's net-zero commitment, together with the capture and storage of residual emissions using carbon dioxide removal (CDR) technologies and a strengthening of nature-based carbon sinks[4].

Enhanced rock weathering (ERW), a CDR strategy based on amending soils with crushed calcium- and magnesium-rich silicate rocks, aims to accelerate natural CO_2 sequestration processes[5–8]. The estimated net global potential for ERW deployed on croplands to draw down CO_2 is substantial, up to $2\,GtCO_2\,yr^{-1}$ (ref. [6]), with co-benefits for production[9–11], soil restoration and ocean acidification[7,8,12]. Agricultural co-benefits can create demand for ERW deployment that is unaffected by diminishing income from carbon-tax receipts generated by other CDR technologies as the transition to clean energy advances and emissions approach net zero[13]. Global action on CDR, and hence progress towards net zero, requires leadership from early-adopting countries through their development of flexible action plans to support policymakers of other nations. Assessment of the contribution of ERW to the United Kingdom's net-zero commitment is therefore required, given that it is a CDR strategy for assisting with decarbonization while improving food production and rebuilding soils degraded by intensified land management[9].

Here we examine in detail the technical potential of ERW implementation on UK arable croplands in a national net-zero context and provide a blueprint by which other nations may proceed with this CDR technology as part of their legislated plans for decarbonization. Using coupled climate–carbon–nitrogen (climate–C–N) cycle modelling of ERW (Methods and Extended Data Fig. 1), we constructed dynamic UK net 2020–2070 C removal budgets and CDR costs after accounting for secondary CO_2 emissions from the ERW supply chain (Methods and Extended Data Fig. 2). Coupled C–N cycle ERW modelling provides the fundamental advance in assessing the effects of cropland N fertilizers on the soil alkalinity balance and mineral weathering kinetics (Methods and Extended Data Fig. 3; Supplementary Information) and ERW-related mitigation of nitrous oxide (N_2O) emissions from agricultural soils[14]. Nitrous oxide is a key long-lived greenhouse gas and important stratospheric-ozone-depleting substance[15]; UK agriculture accounts for 75% of N_2O emissions nationally with high external costs (~£1 billion yr^{-1})[16]. Our analysis, constrained by future energy

[1]Leverhulme Centre for Climate Change Mitigation, School of Biosciences, University of Sheffield, Sheffield, UK. [2]Advanced Resource Efficiency Centre, Management School, University of Sheffield, Sheffield, UK. [3]School of Engineering and Physical Sciences, Heriot-Watt University, Edinburgh, UK. [4]Global Systems Institute, Department of Geography, University of Exeter, Exeter, UK. [5]Cambridge Centre for Energy, Environment and Natural Resource Governance, University of Cambridge, Cambridge, UK. [6]Cambridge Econometrics Ltd, Cambridge, UK. [7]Environment, Earth and Ecosystems, The Open University, Milton Keynes, UK. [8]Understanding Risk Research Group, School of Psychology, Cardiff University, Cardiff, UK. [9]Global Food and Environment Institute, University of Leeds, Leeds, UK. [10]School of Earth and Environment, University of Leeds, Leeds, UK. ✉e-mail: d.j.beerling@sheffield.ac.uk

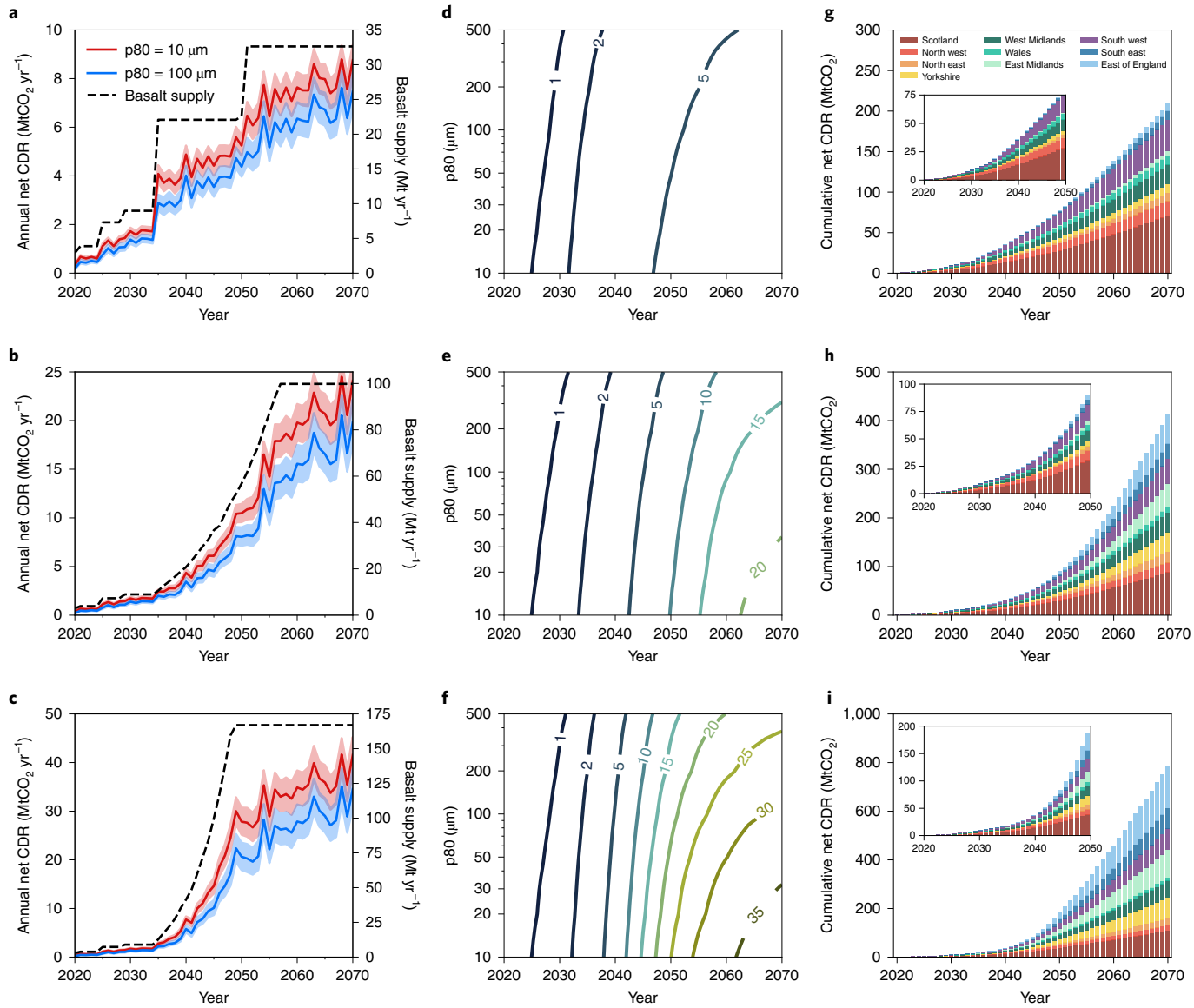

Fig. 1 | Net CDR by ERW deployed on UK arable croplands. a–c, Simulated net CDR (left *y* axis) and annual basalt extraction (right *y* axis) for S1 (**a**), S2 (**b**) and S3 (**c**) resource extraction scenarios. Results are shown for two particle size distributions (p80 = 10 μm diameter and p80 = 100 μm diameter). The shaded envelopes denote 95% confidence limits. **d–f**, Isolines of UK decadal running-average net CDR ($MtCO_2\,yr^{-1}$) for S1 (**d**), S2 (**e**) and S3 (**f**) over time (2020–2070). **a–f** show mean results for three UK-specific basalts. **g–i**, Cumulative net CDR over time for S1 (**g**), S2 (**h**) and S3 (**i**) resource extraction scenarios by UK region, showing the mean of simulations with p80 = 10 μm and p80 = 100 μm and three UK-specific basalts. Insets in **g–i** show the cumulative CDR time series for 2020 to 2050.

policies[17], utilizes basalt as an abundant natural silicate rock suitable for ERW with croplands[9–11], with low- (S1), medium- (S2) and high- (S3) extraction scenarios between 2035 and 2050 (Methods and Extended Data Fig. 4; Supplementary Information).

Patterns of cropland CDR

Across basalt supply scenarios S1 to S3, ERW implementation on arable lands was simulated to remove 6–30 $MtCO_2\,yr^{-1}$ by 2050 (Fig. 1a–c); that is, up to 45% of the CO_2 emissions removal required for UK net-zero emissions (balanced net-zero pathway engineered carbon removal requirement ~58 $MtCO_2\,yr^{-1}$; range 45–112 $MtCO_2\,yr^{-1}$)[4]. Modelled maximum CDR rates were predominantly governed by the geographical extent of ERW application, which increased as resource provision allowed (Fig. 1a–c). Year-on-year legacy effects are also important. CDR rates per unit area increased over time with successive annual applications of rock dust, even if the land area of deployment remained constant. These effects are evident in all scenarios when basalt extraction levelled off, and result from slower-weathering silicate minerals continuing to capture CO_2 in years post-application before they are fully dissolved[6]. By quantifying the geochemical dissolution rates governing ERW and legacy effects, our simulations indicated the CDR potential of ERW rise over time to exceed that suggested by previous mass balance estimates[18–20].

Net-zero pathways for greenhouse gas removal internationally[21], and in the United Kingdom[4], have tended to focus narrowly on bioenergy with carbon capture and storage (BECCS), and direct air carbon capture and storage (DACCS). However, our new results indicate that ERW could be an important overlooked component of national CDR technology net-zero portfolios, working synergistically with croplands, rather than competing with them, as large-scale deployment of BECCS might. In S1, for example, ERW reaches net CDR of 5 $MtCO_2\,yr^{-1}$ by 2050, equalling the DACCS

estimate[5], and closer to 10 $MtCO_2\,yr^{-1}$ by 2060 (Fig. 1a). In the highest resource scenario, S3, ERW delivers approximately half of the net CDR forecast for UK BECCS facilities[5] by 2050 (Fig. 1c).

Milling rocks to fine particle sizes is the most energy-demanding step in the ERW supply chain[18,22]. We therefore assessed a range of options for milled rock particle sizes, as defined by p80 (that is, 80% of the particles have a diameter of less than or equal to the specified value), and the associated energy demands across scenarios S1 to S3 (Fig. 1d–f). For all scenarios, we show that particle size typically has a small effect on net CDR for the first 10–20 years of implementation, as indicated by flat CDR isolines. In the model, ERW deployment locations were prioritized over time, starting from high weathering potential and progressing to low weathering potential. The prioritization of sites with high weathering potential in the first couple of decades means that basalt particles are weathered rapidly regardless of size—a result verified with soil column experiments[23]. In S2, for example, a drawdown of 3 $MtCO_2\,yr^{-1}$ in 2035 with a p80 of 500 µm was achieved only 5 years earlier by milling to a p80 of 10 µm. Our dynamic simulations of temporal ERW carbon budgets, together with recent experimental findings[23], challenge the assumption that rocks must be ground finely to accelerate dissolution for effective CDR[7,8,18,22]. Coarser particles minimize health and safety risks when handling rock dust, in addition to reducing energy demand. However, as S2 and S3 encompass rock dust application on more agricultural land post-2040, with a greater proportion of sub-optimal weathering locations, the dissolution of small particles becomes relevant and the effect of p80 on net CDR increasingly apparent.

Energy requirements for delivering ERW are generally low. Before 2035, the energy demand for rock grinding was minimal across all three scenarios at ~1 TWh yr^{-1}, which is less than 0.2% of the United Kingdom's power production (Extended Data Fig. 5). After 2040, the energy demand for grinding an increased rock mass to be distributed across an expanding area of arable land increased. However, limiting grinding to achieve rock dust with a p80 of 100 µm or more keeps energy demand to less than or equal to 4 TWh yr^{-1}, or 0.6% of UK production for all scenarios. These results mitigate previous concerns that undertaking extensive deployment of ERW in the United Kingdom may compromise energy security[13].

Reducing cumulative CO_2 emissions on the pathway to net zero helps minimize the United Kingdom's contribution to the remaining future carbon budget consistent with keeping warming below a given level[24]. Assuming that ERW practices are maintained between 2020 and 2070, the resulting cumulative net CO_2 drawdown was simulated to be 200, 410, and 800 $MtCO_2$ by 2070 (Fig. 1g–i). Longer-term compensatory ocean outgassing and sediment $CaCO_3$ uptake could reduce net CDR effectiveness by 10–15% by 2070 (Extended Data Fig. 6). Attained over 50 years with ERW, these cumulative CDR ranges compare with an estimated ~696 $MtCO_2$ sequestration over 100 years for afforestation in organic soils of the Scottish uplands[24] and avoids possible soil carbon loss from tree planting[25] and sustained long-term management requirements. More broadly, cumulative ERW-based CDR ranges are comparable to CO_2 removal estimates for UK woodland creation schemes aligned to a balanced net-zero framework (112 $MtCO_2$ by 2050 and ~300 $MtCO_2$ by 2070)[26]. A breakdown of cumulative CDR by region revealed marked shifts in regional contributions from S1 to S3, with increasing contributions over time from croplands in Scotland, northeastern and southwest England, and the Midlands. These regions have acidic soils, where early deployment offers increasing CDR over time from legacy weathering effects. The more aggressive CDR strategy of S3 requires less optimal regions for ERW with the lowest rainfall (southeast and eastern England).

Mapped UK-wide CDR rates per unit area provide fine-scale estimates of modelled carbon removal potential across space and time provide an important tool for precisely targeting ERW interventions (Fig. 2a–c). Results highlight the limited cropland area required for CDR by ERW in the first couple of decades in S1 and S2, and the rise in CDR per unit area over time. Across all decades and scenarios, our geospatial net CDR estimates typically exceed those for the low-carbon farming practices forming part of net-zero pathways for agriculture[4], including switching to less intensive tillage (typically ~1 $tCO_2\,ha^{-1}\,yr^{-1}$)[27], conversion of arable land to ley pasture (~1–5 $tCO_2\,ha^{-1}\,yr^{-1}$)[28] and inclusion of cover crops in cropping systems (1.1 ± 0.3 $tCO_2\,ha^{-1}\,yr^{-1}$)[29].

Underlying the geospatial maps of net CDR are strong cycles in alkalinity generation and soil pH, and intra-annual dissolution/precipitation of soil carbonates, driven by seasonal climate and crop production effects (Extended Data Fig. 7). These results show a decline in the periodic dissolution of soil (pedogenic) carbonates over decades as the cumulative effect of alkalinity systematically raises the seasonal minimum in soil pH and drives a steady increase in the net CDR per unit area each year. Rising alkalinity over time increases the soil buffer capacity, which reduces the risk of pH reversal, thereby improving security of CO_2 storage. These results for the UK maritime climate are consistent with soil carbonate accumulation and persistent in arid systems[30], and highlight the challenge of monitoring, reporting and verifying CDR via seasonal dynamics of soil carbonates, and soil fluid alkalinity discharge, over multiple field seasons.

Costs of cropland CDR

The costs of CDR must be known to evaluate commercial feasibility, permit comparison with other CDR technologies and allow governments to understand the carbon price required to pay for it. Between 2020 and 2070, CDR costs fall from £200–250 $tCO_2^{-1}\,yr^{-1}$ in 2020 to £80–110 $tCO_2^{-1}\,yr^{-1}$ by 2070 (Fig. 2a–c). Modelled longer-term cost trends are driven by rising CDR with successive rock dust applications (Fig. 1a–c) and declining renewable energy prices (Methods and Extended Data Fig. 8). Grinding rocks to smaller particle sizes carries a minor financial penalty. As the geographical deployment of ERW increases in S3, the price of CDR rises from 2030 to 2050 due to higher total energy costs associated with grinding more rock and the requirement for more extensive logistical operations, particularly spreading of the rock dust over farms. However, it subsequently falls as CDR rates increase with repeated rock dust applications (Fig. 1). The dominant cost elements are electricity for rock grinding and fuel for spreading the milled rock on farmland (Fig. 3d–f). Mineral P and K nutrient fertilizers are expensive (£300–400 t^{-1} and £250–300 t^{-1} for P and K fertilizers, respectively)[31]. Given fertilizer application rates per unit of land area typical for arable crops (Extended Data Fig. 9), using basalt could provide savings sufficient to cover transport costs (Fig. 3d–f).

Modelled average CDR costs for ERW practices are towards the lower end of the range for BECCS, which varies widely across sectors[4] (£70–275 tCO_2^{-1}), and half of that estimated for early-stage DACCS plants. DACCS CDR has an indicative price of £400 tCO_2^{-1} during the 2020s and £180 tCO_2^{-1} by 2050 as the technology develops and scales up globally[4,21]. ERW is thus competitive relative to industrial CDR technologies such as these that will also be required to help achieve net-zero emissions.

Fine-scale spatial and temporal assessment of CDR costs (Fig. 4a–c), combined with analysis of regional CO_2 drawdown (Fig. 2a–c), informs geographical prioritization of near-term opportunities for rapid ERW deployment and public consultations on these activities. Costs in all scenarios decrease through time as CDR rises, with geographical variations in CDR costs approximately twofold by 2050–2060. These patterns reflect differences in CDR and, to a lesser extent, transport distances between source rocks and croplands. By 2060–2070, the lowest costs (£75–100 tCO_2^{-1}) occur in the northeast of England, the Midlands and Scotland, where CDR rates are highest because of favourable soil weathering environments and regional climate effects on site water balance (precipitation minus evapotranspiration).

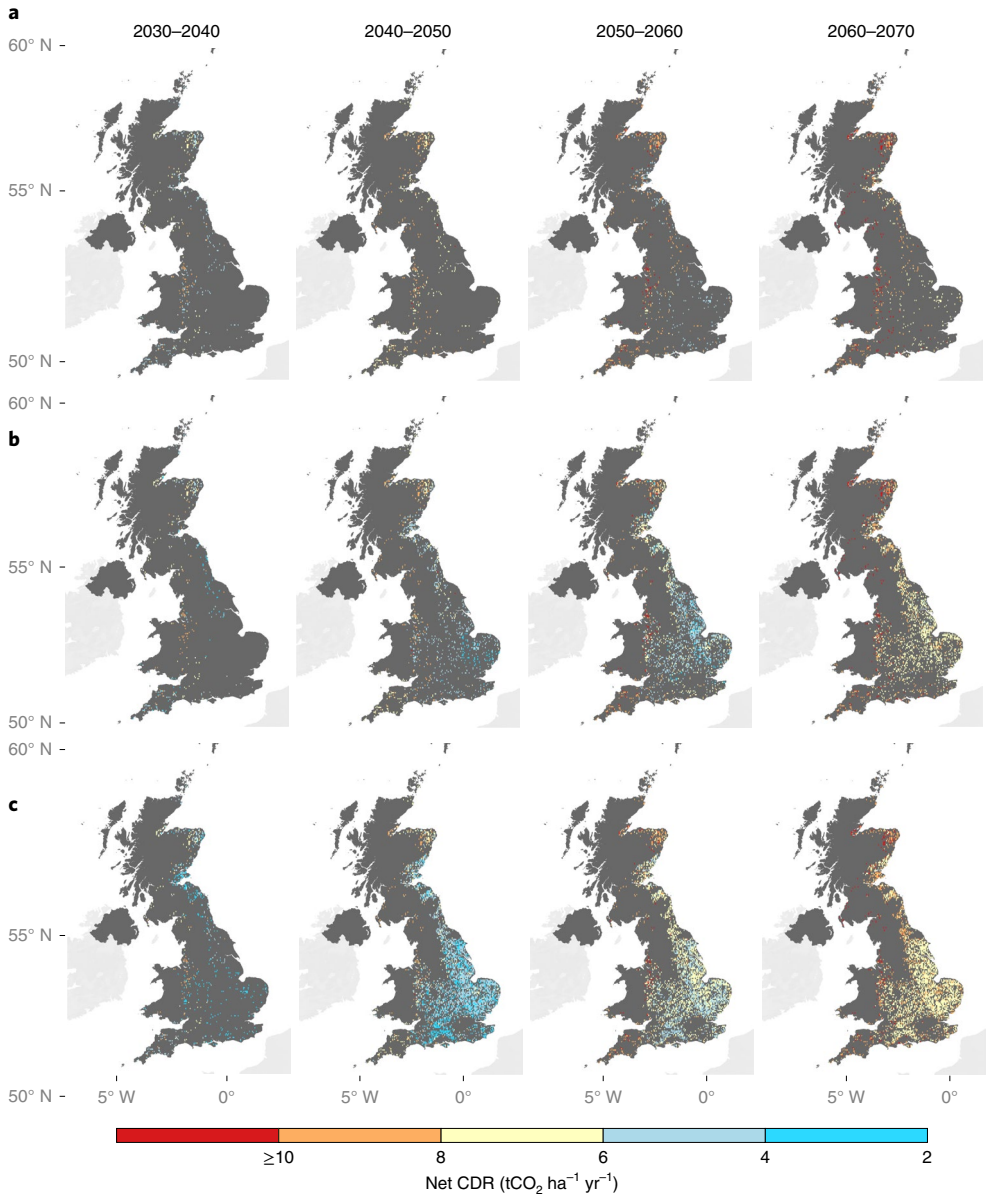

Fig. 2 | Mapped fine-scale decadal average UK net CDR. a–c, Mapped net CDR from ERW deployed on arable croplands for S1 (**a**), S2 (**b**) and S3 (**c**) resource extraction scenarios is shown for the decades indicated. The mean of simulations with p80 = 10 μm and p80 = 100 μm and three UK-specific basalts is shown.

Nations committing to net-zero targets require carefully designed economic and policy frameworks to incentivize uptake and cover the costs of CDR technologies[13,21], as well as the modification of existing emissions trading schemes. Costs might be met in the near term through farming subsidies; agriculture is heavily supported in most countries worldwide[13]. Actions to enhance soil carbon storage are already subsidized in the United States, and European proposals to incentivize CDR by farmers are underway[32]. Redesigned agricultural policies in the United Kingdom post-Brexit aim to provide public funding to support farmers in delivering environmental public goods and contributing to net-zero emissions[33] by 2050. Identifying strategic options, such as ERW, with multiple co-benefits for agricultural productivity and the environment is key to enhancing uptake.

Co-benefits of ERW for agriculture

Arable soils are a critical resource supporting multiple ecosystem services, and the adoption of ERW into current agricultural practices could enhance soil functions. We quantified three major soil-based co-benefits with the potential to increase the demand for early deployment of the technology: reducing excess soil acidity, increasing the primary supply of fertilizer-based mineral nutrients (P and K)[5,9,10] and mitigating soil N_2O fluxes[14].

Soil acidity (that is, pH below 6.5)[34] limits yields and correction is essential for good soil management, crop growth, nutrient use efficiency and environmental protection[35]. Following initialization with topsoil (0–15 cm) pH values based on high-resolution field datasets (Methods), the implementation of ERW reduces the fraction of arable soils with pH less than 6.5 in England to 13% by 2035 (S1), and completely by 2045 and 2055 in S2 and S3, respectively (Fig. 5a). In Scotland, where agricultural soils are more acidic than in England, the co-benefit of ERW in raising soil pH could be considerable, with reductions to 10% by 2050 in S1 and eliminating acidic soils by 2045–2050 in S2 and S3 (Fig. 5b). Reversing soil acidification across England and Scotland

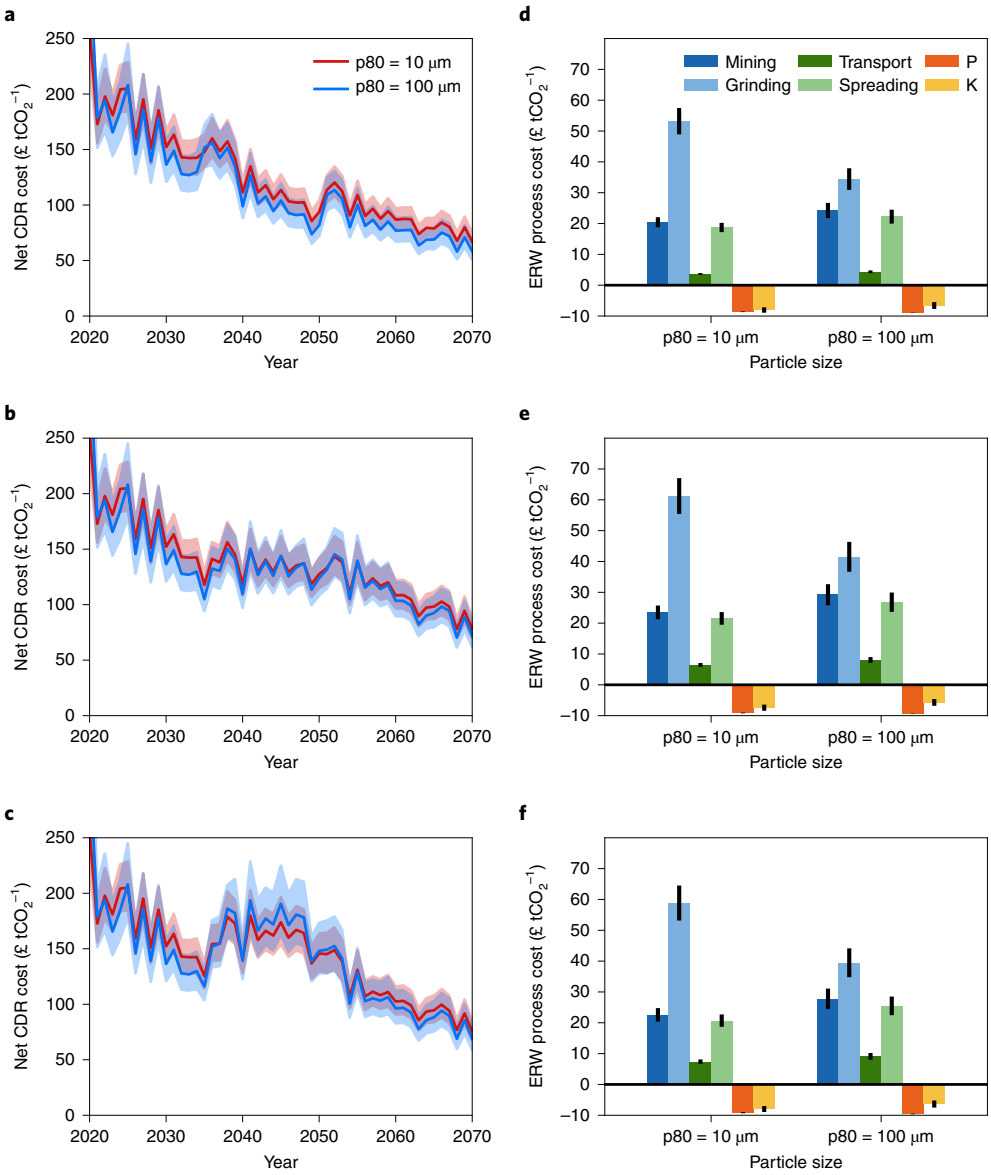

Fig. 3 | Costs of CDR by ERW deployed on UK arable croplands. a–c, Costs of net CDR for S1 (**a**), S2 (**b**) and S3 (**c**) resource extraction scenarios over time (2020–2070). Results are shown for two particle size distributions (p80 = 10 μm and p80 = 100 μm). The shaded envelopes denote 95% confidence limits. **d–f**, Breakdown of ERW processes contributing to CDR costs, including savings resulting from basalt substituting for P and K fertilizers averaged for 2060–2070 under S1 (**d**), S2 (**e**) and S3 (**f**). Error bars indicate 95% confidence limits. All panels display average results for three UK-specific basalts.

could increase nutrient uptake to boost yields on underperforming croplands[34,35], lower the potential for metal toxicity[10] at low pH and enhance N fixation by legumes[36]. Calcium released by ERW can also stimulate root growth and water uptake[37] and multi-element basalt can fortify staple crops such as cereals with important micronutrients, including iron and zinc[9]. Raising soil pH with widespread ERW practices in the United Kingdom, and elsewhere, to improve agricultural productivity[38] releases land for additional CDR opportunities, including afforestation and bioenergy cropping[4,21].

Calculated rates of inorganic P and K nutrient supply for crops via ERW of basalt are comparable to typical P and K fertilizer application rates for major tillage crops (Extended Data Fig. 9). ERW with basalt could therefore substantially reduce the reliance of agriculture on the expensive and finite rock-derived sources of P and K fertilizers required to support increased agricultural production over the next 50 years in the United Kingdom, and globally, to meet the demands of a growing human population[39]. Reductions in P and K fertilizer usage lower unintended environmental impacts, supply chain CO_2 emissions and costs. For the United Kingdom, assuming that annual fertilizer application on ERW cropland areas in S1–S3 to replenish pools of P and K is reduced, the avoided carbon emissions are estimated to be 0.1–1 $MtCO_2\,yr^{-1}$, with maximum cost savings of £100–700 million yr^{-1} by 2070 (Fig. 5c–f). However, we note that not all crops require annual fertilization. These savings could contribute to offsetting the cost of undertaking ERW practices, but may be reduced by precision farming techniques, including applying variable levels of fertilizers within fields, and controlled-release fertilizers.

Practices that optimize the efficient use of N on croplands to reduce N_2O emissions from soils are important for ambitious net-zero agriculture pathways in the United Kingdom[4]. Our process-based model simulations, calibrated with field data[14], indicate that ERW deployment on UK croplands could reduce soil N_2O emissions by ~0.1 Mt of

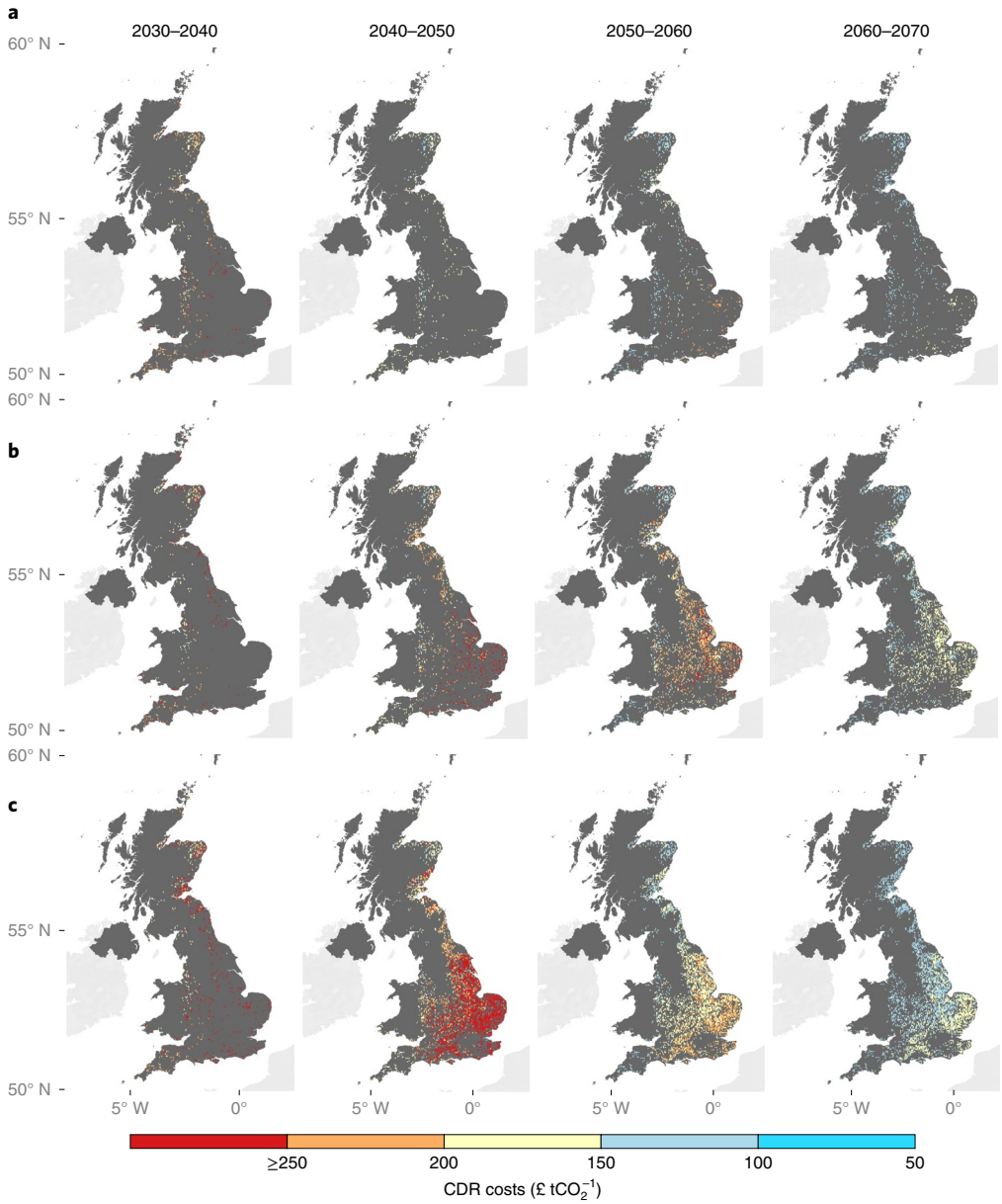

Fig. 4 | Mapped fine-scale decadal average UK net CDR costs. a–c, Mapped net CDR costs of ERW deployed on arable croplands for SI (**a**), S2 (**b**) and S3 (**c**) resource extraction scenarios for the decades indicated. The mean of simulations with p80 = 10 μm and p80 = 100 μm and three UK-specific basalts is shown.

CO_2 equivalent (CO_2e) per year, ~1 MtCO_2e yr^{-1} and ~1.5 MtCO_2e yr^{-1} by 2070 in S1, S2 and S3, respectively (Fig. 5e); this equates to a reduction of up to 20% relative to croplands in 2010 (Fig. 5f). This contrasts with large-scale land-based CDR strategies for increasing soil organic carbon stocks, which can increase soil N_2O emissions[40]. ERW may therefore offer a new management option for mitigating soil N_2O fluxes that is comparable in magnitude to other proposed abatement measures[41] with the additional win of CDR.

Societal and community acceptability

Societal acceptance of ERW practices is needed on all scales, from the national-political to local community and individual farm scales. 'Acceptance' in this context should be regarded not as an absolute mandate to proceed, but instead as recognition of the need to work with stakeholders and affected publics to identify the conditions under which this technology might proceed[42]. Additional mining operations with unintended environmental impacts raise particular sensitivities[42] and two of our scenarios (S2 and S3) require new mines to be established between 2035 and 2050 to provide basalt; increases post-2035 account for delays due to complex licensing procedures (Extended Data Fig. 4). Concentrating resource production at larger sites (~1 Mt basalt yr^{-1}) requires annual increases in mine numbers of 6% (S2) and 13% (S3); smaller mines (~250 kt yr^{-1}) necessitate larger annual increases (Supplementary Information). However, the scale-up rate is less than the historical 10-year maximum (1960–1970) and limited to 15 years. Recycling the United Kingdom's annually produced calcium silicate construction and demolition waste (~80 Mt yr^{-1})[43], which has potential to substitute for basalt[6], could substantially reduce mined resource demand by between 80% (S2) and 45% (S3).

Traditional mining operations provide local employment opportunities but have encountered controversy nonetheless because of

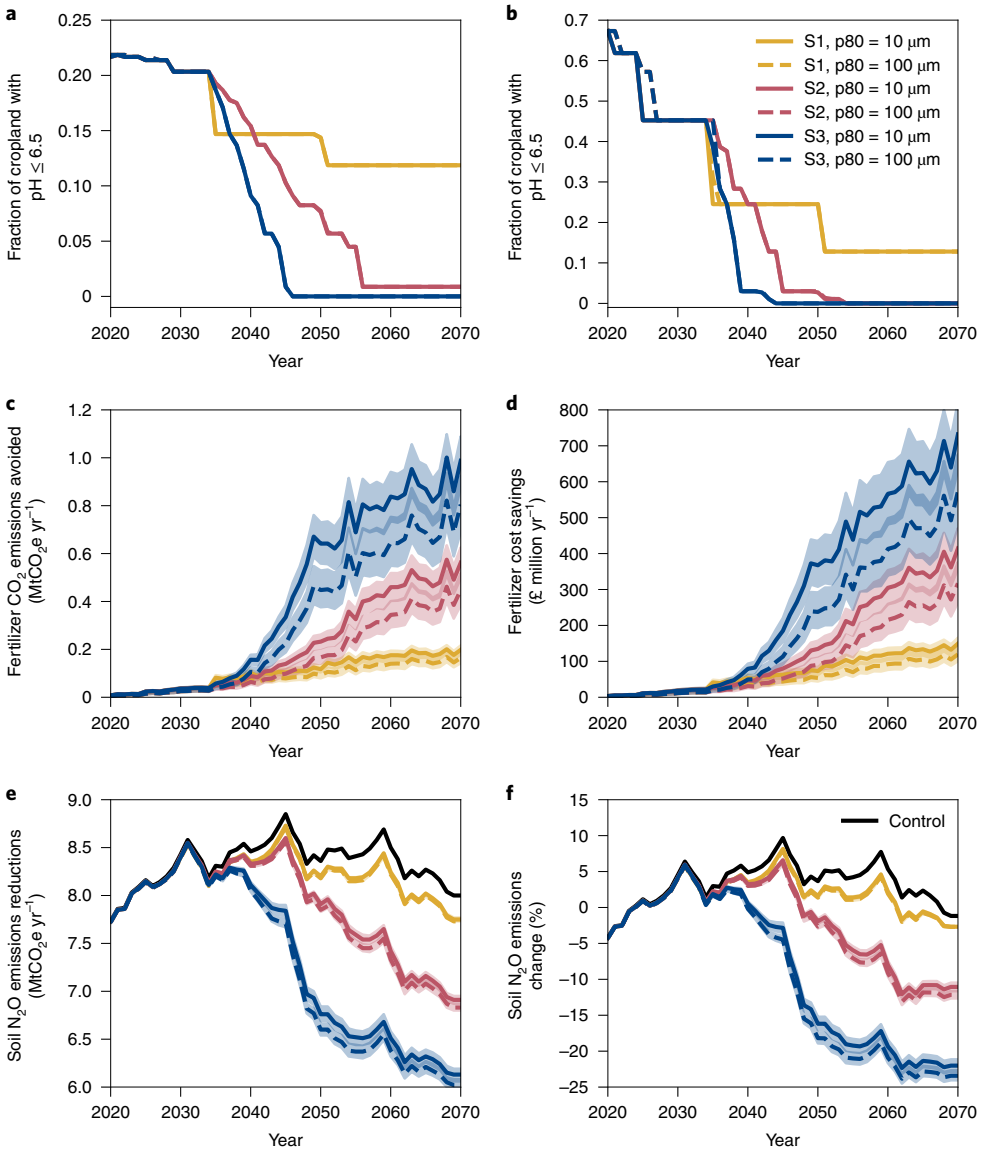

Fig. 5 | Agricultural ecosystem co-benefits of ERW. a,**b**, Reduction in the fraction of acidic land in England (**a**) and Scotland (**b**) following deployment of ERW. **c**,**d**, CO_2 emissions avoided (**c**) and cost savings (**d**) resulting from using basalt to substitute for P and K fertilizers. **e**,**f**, Soil N_2O emissions reductions from croplands (**e**) and percentage change from 2010 (**f**) following ERW deployment. N_2O results are shown as 10 yr annual running averages. The black line in **f** and **g** denotes results of the control 'no basalt' simulations. Results are shown for S1, S2 and S3 resource extraction scenarios in all panels, with the line style indicating the particle size distribution (p80 = 10 μm and p80 = 100 μm); the legend in **b** applies to all panels. The shaded envelopes denote 95% confidence limits.

concerns about sustainability, community impacts and local health and environmental risks[44]. Mining operations to enhance national carbon sequestration may raise different ethical and risk–benefit narratives[45]. Procedural and distributional fairness in siting mines, alongside long-term proactive engagement with the communities likely to be affected by any new mining operations, will be critical for acceptance[44], together with sustainable management plans for quarry restoration post-extraction[46,47]. The issue of mining new materials for CDR is part of a wider debate regarding the sustainability of increasing resource extraction for green technologies, such as electric vehicles or photovoltaic cells. Achieving this at scale requires the development of innovative solutions that combine improved resource efficiency and use of waste mining products, circular economy production systems and extraction efforts focused primarily in the regions or countries where materials are to be used[48]. Although nature-based techniques for CDR (for example forestry, carbon sequestration in soils) are likely to be preferred by public groups over engineered technologies[42,49], they are unlikely to be sufficient to deliver net-zero emissions nationally or globally. Above all, broad societal support is unlikely to be forthcoming unless ERW is developed alongside an ambitious portfolio of conventional climate mitigation policies[49].

Implications for ERW deployment

Our analysis with dynamic ERW carbon budget modelling suggests that this technically straightforward-to-implement CDR technology could prove transformative for utilizing agriculture to mitigate climate change[6,9,10] and play a larger role in national CDR portfolio programmes than previously realized. Unlike industrial CDR processes, including BECCS or DACCS, ERW could be rolled out without major new industrial infrastructure, and incentivized through amended agricultural subsidy frameworks. We show that

eliminating the energy-demanding requirement for milling rocks to fine particle sizes requires early and sustained implementation of ERW practices, subject to public acceptance. This has the additional important advantages of maximizing CDR and lowering costs to a highly competitive price of £80–110 $tCO_2^{-1}yr^{-1}$ by 2070. Our findings underscore the urgent need for long-term field trials across a range of agricultural systems to evaluate this technology with empirical evidence, alongside monitoring of potential unintended negative consequences[9,50]. High-resolution geospatial ERW assessments provide a detailed basis for mapping out routes to technological development and afford opportunities to minimize social and economic barriers by identifying priority regions for public engagement. Scaling up ERW in the United Kingdom and other G20 nations will require funding, public support, regulation and governance to ensure sustainability, and a stable policy framework[4,13] to accelerate global CDR goals with agriculture[6,9,10] as the world transitions to net-zero emissions.

Online content

Any methods, additional references, Nature Research reporting summaries, source data, extended data, supplementary information, acknowledgements, peer review information; details of author contributions and competing interests; and statements of data and code availability are available at https://doi.org/10.1038/s41561-022-00925-2.

Received: 3 June 2021; Accepted: 1 March 2022;
Published online: 25 April 2022

References

1. *Global Climate Action Portal* (UNFCCC, accessed 2021); https://climateaction.unfccc.int
2. Hansen, J. et al. Assessing "dangerous climate change": required reduction of carbon emissions to protect young people, future generations and nature. *PLoS ONE* **8**, e81648 (2013).
3. *Greenhouse Gas Removals—Call for Evidence* (HM Government, 2020).
4. *The Sixth Carbon Budget: The UK's Path to Net Zero* (Committee on Climate Change, 2019).
5. Hartmann, J. et al. Enhanced chemical weathering as a geoengineering strategy to reduce atmospheric carbon dioxide, supply nutrients, and mitigate ocean acidification. *Rev. Geophys.* **51**, 113–149 (2013).
6. Beerling, D. J. et al. Potential for large-scale CO_2 removal via enhanced rock weathering with croplands. *Nature* **583**, 242–248 (2020).
7. Kohler, P., Hartman, J. & Wolf-Gladrow, D. A. Geoengineering potential of artificially enhanced silicate weathering of olivine. *Proc. Natl Acad. Sci. USA* **107**, 20228–20233 (2010).
8. Taylor, L. L. et al. Enhanced weathering strategies for stabilizing climate and averting ocean acidification. *Nat. Clim. Change* **6**, 402–406 (2016).
9. Beerling, D. J. et al. Farming with crops and rocks to address global climate, food and soil security. *Nat. Plants* **4**, 138–147 (2018).
10. Kantola, I. B. et al. Potential of global croplands and bioenergy crops for climate change mitigation through deployment for enhanced weathering. *Biol. Lett.* **13**, 20160714 (2017).
11. Kelland, M. E. et al. Increased yield and CO_2 sequestration potential with the C_4 cereal *Sorghum bicolor* cultivated in basaltic rock dust-amended agricultural soil. *Glob. Change Biol.* **26**, 3658–3676 (2020).
12. Vakilifard, N. et al. The role of enhanced weathering deployment with agriculture in limiting future warming and protecting coral reefs. *Environ. Res. Lett.* **19**, 094005 (2021).
13. Cox, E. & Edwards, N. R. Beyond carbon pricing: policy levers for negative emissions technologies. *Clim. Policy* **19**, 1144–1156 (2019).
14. Blanc-Betes, E. et al. In silico assessment of the potential of basalt amendments to reduce N_2O emissions from bioenergy crops. *Glob. Change Biol. Bioen.* **13**, 224–241 (2021).
15. Reay, D. S. et al. Global agriculture and nitrous oxide emissions. *Nat. Clim. Change* **2**, 410–416 (2012).
16. Bhunnoo, R. & Poppy, G. M. A national approach for transformation of the UK food system. *Nat. Food* **1**, 6–8 (2020).
17. Holden, P. B. et al. Climate-carbon cycle uncertainties and the Paris Agreement. *Nat. Clim. Change* **8**, 609–613 (2018).
18. Renforth, P. The potential of enhanced weathering in the UK. *Int. J. Greenh. Gas. Cont.* **10**, 229–243 (2012).
19. Smith, P., Haszeldine, R. S. & Smith, S. M. Preliminary assessment of the potential for, and limitations to, terrestrial negative emissions technologies in the UK. *Environ. Sci. Process. Impacts* **18**, 1400–1405 (2016).
20. Royal Academy of Engineering *Greenhouse Gas Removal Technologies* (The Royal Society, 2018).
21. IPCC *Special Report on Global Warming of 1.5 °C* (eds Masson-Delmotte, V. et al.) (WMO, 2018).
22. Moosdorf, N., Renforth, P. & Hartmann, J. Carbon dioxide efficiency of terrestrial weathering. *Environ. Sci. Technol.* **48**, 4809–4816 (2014).
23. Hartmann, J. & Amann, T. Limits of weathering potentials—deductions from column experiments. In *Goldschmidt 2021* (European Geophysical Union, 2021); https://2021.goldschmidt.info/goldschmidt/2021/meetingapp.cgi/Paper/6179
24. Fletcher, T. I. et al. The carbon sequestration potential of Scottish native woodland. *Environ. Res. Commun.* **3**, 041003 (2021).
25. Friggens, N. L. et al. Tree planting in organic soils does not result in net carbon sequestration on decadal timescales. *Glob. Change Biol.* **26**, 5178–5188 (2020).
26. Bradfer-Lawrence, T. et al. The potential contribution of terrestrial nature-based solutions to a national 'net zero' climate target. *J. Appl. Ecol.* https://doi.org/10.1111/1365-2664.14003 (2021).
27. Powlson, D. S. et al. Limited potential of no-till agriculture for climate change mitigation. *Nat. Clim. Change* **4**, 678–683 (2014).
28. Ostle, N. J., Levy, P. E., Evans, C. D. & Smith, P. UK land use and soil carbon sequestration. *Land Use Policy* **26S**, S274–S283 (2009).
29. Poeplau, C. & Don, A. Carbon sequestration in agricultural soils via cultivation of cover crops—a meta-analysis. *Agric. Ecosyst. Environ.* **200**, 33–41 (2015).
30. Zamanian, K., Pustovoytov, K. & Kuzyakov, Y. Pedogenic carbonates: forms and formation processes. *Earth Sci. Rev.* **157**, 1–17 (2016).
31. *GB Fertiliser Prices* (Agriculture and Horticulture Development Board, 2020); https://ahdb.org.uk/GB-fertiliser-prices
32. Schenuit, F. et al. Carbon dioxide removal policy in the making: assessing developments in 9 OECD cases. *Front. Clim.* **3**, 638805 (2021).
33. Clements, J. et al. How can academic research on UK agri-environmental schemes pivot to meet the addition of climate mitigation aims? *Land Use Policy* **106**, 105441 (2021).
34. Goulding, K. W. T. Soil acidification and the importance of liming, agricultural soils with particular reference to the United Kingdom. *Soil Use Manag.* **32**, 390–399 (2016).
35. Holland, J. E. et al. Liming impacts on soils, crops and biodiversity in the UK: a review. *Sci. Total Environ.* **610-611**, 316–332 (2018).
36. Alves, L. A. et al. Biological N_2 fixation by soybeans grown with and without liming on acid soils in a no-till integrated crop-livestock system. *Soil Till. Res.* **209**, 104923 (2021).
37. Lynch, J. P. & Wojciechowski, T. Opportunities and challenges in the subsoil: pathways to deeper rooted crops. *J. Exp. Bot.* **66**, 2199–2210 (2015).
38. Lerhmann, J. & Possinger, A. Atmospheric CO_2 removal by rock weathering. *Nature* **583**, 205–205 (2020).
39. Amundson, R. et al. Soil and human security in the 21st century. *Science* **348**, 126107-1 (2015).
40. Guenet, B. et al. Can N_2O emissions offset the benefits from soil organic carbon storage?. *Glob. Change Biol.* **27**, 237–256 (2020).
41. Rees, R. M. et al. Nitrous oxide mitigation in UK agriculture. *Soil Sci. Plant Nutr.* **59**, 3–15 (2013).
42. Cox, E., Spence, E. & Pidgeon, N. Public perceptions of carbon dioxide removal in the United States and the United Kingdom. *Nat. Clim. Change* **10**, 744–749 (2020).
43. Department for Communities and Local Government *Survey of Arisings and Use of Alternatives to Primary Aggregates in England: Construction, Demolition and Excavation Waste* (Crown Estates, 2007).
44. Moffat, K. et al. in *Mining and Sustainable Development: Current Issues* (ed. Lodhia, S.) 45–62 (Routledge, 2018).
45. Cox, E., Pidgeon, N. F., Spence, E. M. & Thomas, G. Blurred lines: the ethics and policy of greenhouse gas removal at scale. *Front. Environ. Sci.* **6**, 38 (2018).
46. Bradshaw, A. Restoration of mined lands—using natural processes. *Ecol. Eng.* **8**, 255–269 (1997).
47. Novak, J. & Prach, K. Vegetation succession in basalt quarries: pattern on a landscape scale. *Appl. Veg. Sci.* **6**, 111–116 (2003).
48. Herrington, R. Mining our green future. *Nat. Rev. Mater.* **6**, 456–458 (2021).
49. Wolske, K. S. et al. Public support for carbon dioxide removal strategies: the role of tampering with nature perceptions. *Climatic Change* **152**, 345–361 (2019).
50. Edwards, D. P. et al. Climate change mitigation: potential benefits and pitfalls of enhanced rock weathering in tropical agriculture. *Biol. Lett.* **13**, 20160715 (2017).

Methods

Resource extraction scenarios. Under S1, per-capita production of aggregates continues to fall from 1.9 to 1.5 t yr^{-1} by 2032 and remains constant thereafter, with the spare capacity used and ramped up for ERW. Under S2, rock extraction is scaled up by 7% (half the historical maximum rate of increase) until the total additional capacity is equal to the maximum historical value in 1990 (100 Mt yr^{-1}). Under S3, rock extraction is scaled up by 15% (that is, historical annual 10-yr rolling average) until the additional capacity is 160 Mt yr^{-1}; that is, equivalent to the total increase in the UK crushed rock supply post-1945 (Supplementary Information). Extraction of resources scales at rates compatible with historical patterns (Extended Data Fig. 4) and those advanced for delivering CDR by BECCS (and its supply chains) and DACCS[4].

Soil profile ERW modelling. Our analysis used a one-dimensional vertical reactive transport model for rock weathering with steady-state flow and transport through a series of soil layers. The transport equation included a source term that represents rock grain dissolution within the soil profile[4] with advancements to incorporate the effects of the biogeochemical transformations of N fertilizers (Supplementary Information). The core model accounted for changing dissolution rates with soil depth and time as grains dissolve, chemical inhibition of dissolution as pore fluids approach equilibrium with respect to the reacting basaltic mineral phases, and the formation and dissolution of pedogenic calcium carbonate mineral in equilibrium with pore fluids[4]. Simulations considered UK basalts with specified mineralogies from three commercial quarries (Supplementary Information).

We modelled the ERW of a defined particle size distribution (psd) with theory developed previously[4]. As the existing psds at each soil layer are at different stages of weathering, the combined psd at each level, and for each mineral, was calculated and tracked over time[4]. We accounted for repeated basalt applications by combining the existing psd with the psd of the new application. Simulated mineral dissolution fluxes from the model output were used to calculate the release of P and K over time. Mass transfer of P within the relatively more rapidly dissolving[51] accessory mineral apatite was calculated on the basis of the P content of the rock and the volume of bulk minerals dissolved during each time step.

The mathematical model combined a multi-species geochemical transport model with a mineral mass balance and rate equations for the chemical dissolution of basaltic mineral phases. The model included an alkalinity mass balance that incorporated the effect of fertilizer applications and soil N cycling and dynamic calculations of pH in soil pore waters. The main governing equations are detailed below.

Transport equation. The calculated state variable in the transport equation is the dissolved molar equivalents of elements released by stoichiometric dissolution of mineral i, in units of mol l^{-1}; ϕ is the volumetric water content, C_i is the dissolved concentration (in mol l^{-1}) of mineral i transferred to solution, t is time (months), q is vertical water flux (m y^{-1}), z is the distance along the vertical flow path (m), R_i is the weathering rate of basalt mineral i (mole per litre of bulk soil month^{-1}) and C_{eqi} is the solution concentration of weathering product at equilibrium with the mineral phase i (equation (1)). Values for C_{eqi} for each of the mineral phases in the basalt grains were obtained by calibrating the results of the performance model against those of a 1D reactive transport model, as described previously[4].

Rates of basalt grain weathering defined the source term for weathering products and were calculated as a function of soil pH, soil temperature, soil hydrology, soil respiration and crop net primary productivity. The vertical water flux was zero when pore water content was below a critical threshold for vertical flow. Weathering occurred under no-flow conditions and the accumulated solutes in pore water were then advected when water flow was initiated under sufficient wetting, tracked using a single bucket model.

$$\phi \frac{\partial C_i}{\partial t} = -q \frac{\partial C_i}{\partial z} + R_i \left(1 - \frac{C_i}{C_{eqi}}\right) \quad (1)$$

Mineral mass balance. The change in mass of basalt mineral i, B_i, is defined by the rate of stoichiometric mass transfer of mineral i elements to solution. Equation (2) is required because we considered a finite mass of weathering rock, which over time could react to completion, either when solubility equilibrium between minerals and pore water composition was reached, or when applied basalt was fully depleted.

$$\frac{\partial B_i}{\partial t} = -R_i \left(1 - \frac{C_i}{C_{eqi}}\right) \quad (2)$$

Removal of weathering products. The total mass balance over time (equation (3)) for basalt mineral weathering allows calculation of the products transported from the soil profile. The total mass of weathering basalt is defined as follows where m is the total number of weathering minerals in the rock, T is the duration of weathering and L is the total depth of the soil profile (in m). We define q, the vertical water flux, as the net monthly sum of water from precipitation and irrigation, minus evapotranspiration, as calculated by the Community Land Model v.5 (CLM5).

$$\text{Total weathered basalt} = \sum_{i=1}^{m} \phi \int_{z=0}^{L} C_i(t,z)\,\mathrm{d}z + q \int_{t=0}^{T} C_i(t,L)\,\mathrm{d}t \quad (3)$$

Coupled climate–C–N cycle ERW simulations. Our model simulation framework (Extended Data Fig. 1) started with future UK climates (2020–2070) from the medium-mitigation future pathway climate (Shared Socioeconomic Pathway (SSP) 3-7.0) ensemble of Coupled Model Intercomparison Project Phase 6 (CMIP6) runs with the Community Earth System Model v.2. Future climates were used to drive CLM5 to simulate at high spatial resolution (23 km × 31 km) and high temporal resolution (30 min) terrestrial C and N cycling with prognostic crop growth and other ecosystem processes, including heterotrophic respiration[52,53] (Supplementary Information). CLM5 simulates monthly crop productivity, soil hydrology (precipitation minus evapotranspiration), soil respiration and N cycling. CLM5 includes representation of eight crop functional types, each with specific ecophysiological, phenological and biogeochemical parameters[52,53]. CLM5 includes CO_2 fertilization effects on agricultural systems benchmarked against experiments and observations[54,55]. An atmospheric CO_2 increase of ~200 ppm from 2015 to 2070 is defined by SSP3-7.0. In our CLM5 simulations with rising CO_2 and climate change, wheat net primary productivity increased by 8%, evapotranspiration decreased by 21% and water-use efficiency increased by 25% (Supplementary Information). Both increasing net primary productivity and decreasing evapotranspiration can facilitate weathering in our soil profile ERW model (Supplementary Information). We initialized CLM5 simulations for 2010 using fully spun-up conditions from global runs at ~100 km × 100 km resolution, adding an extra 60 yr spin-up in the regional set-up to stabilize the C and N pools to the higher-resolution setting.

CLM5 includes an interactive N fertilization scheme that simulates fertilization by adding N directly to the soil mineral N pool to meet crop N demands using both synthetic fertilizer and manure application[52,53]. Synthetic fertilizer application was prescribed by crop type and varied spatially for each year based on the Land Use Model Intercomparison Project and land-cover change time series (Land-Use Harmonization 2 for historical rates and SSP3 for future rates)[55,56]. N fertilizer rates increased by 18% per decade from 2020 to 2050 in agreement with the United Kingdom's Committee on Climate Change forecasts of future N fertilizer usage[57], and then stabilized from 2050 to 2070. Average UK CLM5 fertilizer application rates (148 kg N ha^{-1} yr^{-1}) are consistent with current practices[58]. Organic fertilizer was applied at a fixed rate (20 kg N ha^{-1} yr^{-1}) throughout the simulations.

CLM5 tracks N content in soil, plant and organic matter as an array of separate N pools and biogeochemical transformations, with exchange fluxes of N between these pools[52,53]. The model represents inorganic N transformations based on the DayCent model, which includes separate dissolved NH_4^+ and NO_3^- pools, as well as environmentally controlled nitrification, denitrification and volatilization rates[59]. To model the effect of basalt addition on fluxes of N_2O from soil, we included the updated denitrification DayCent module[14], modified to capture the soil pH ranges in UK croplands. The possible effect of increased soil pH from basalt application increasing NH_3 volatilization and, indirectly, N_2O emissions, was not explicitly modelled. However, the error term is likely to be small, given that it accounts for less than 5% of total agricultural N_2O emissions[60,61]. Cropland CLM5 soil N emissions are within the range of estimates in UK croplands based on bottom-up inventories and other land surface models, with N_2O fluxes showing broad similarities in terms of regional patterns and magnitude with the UK National Atmospheric Emission Inventory (Supplementary Information).

Modelling soil N effects on ERW. The inclusion of mechanistic simulation of N cycling processes coupled to ERW via 16 stoichiometric N transformations that influence the soil weathering environment represents a theoretical advance over previous modelling (Supplementary Information). The modelling accounts for 20 depths (20 soil layers) in the soil profile at each location with a monthly time step; the variables passed from CLM5 by time and depth to the 1D ERW model are given in the Supplementary Information. At each depth, we computed N transformation effects on soil water alkalinity with reaction stoichiometries that added or removed alkalinity. Together with soil CO_2 levels, this affected pore water pH and the aqueous speciation that determined mineral weathering rates. This modelling advance allowed us to mechanistically account for the impact of N fertilization (which is recognized to potentially lead to nitric acid-dominated weathering[62,63] at low pH with no C capture) of cropland on basalt weathering rates. Dynamic modelling at monthly time steps resolved seasonal cycles of CDR via alkalinity fluxes and soil carbonate formation/dissolution in response to future changes in atmospheric CO_2, climate, land surface hydrology, and crop and soil processes.

The effect of the N cycle on the soil acidity balance (Extended Data Fig. 3) was derived from N transformations associated with the production or consumption of hydrogen ions (Supplementary Information). We assigned a stoichiometric acidity flux $\Delta H_{i,N}$ (mol H^+ mol^{-1} N) to each N flux $F_{i,N}$ (g N m^{-3} soil s^{-1}) calculated by the CLM5 code (Supplementary Information). The product ($F_{i,N}\Delta H_{i,N}$), with

appropriate unit conversions, gives the acidity flux during the time step Δt (s month^{-1}) for the ith reaction of the CLM5 N cycle. Their sum (equation (4)) is, therefore, the total change in acidity $\Delta\text{Acidity}_N$ due to the CLM5 N cycle:

$$\Delta\text{Acidity}_N = \sum (F_{i,N}\Delta H_{i,N})/14.0067\Delta t \quad (4)$$

where 14.0067 g N mol^{-1} N is the atomic weight of N and the time step is one month. Along with the Ca, Mg, K and Na ions released from weathering the applied minerals, $\Delta\text{Acidity}_N$ contributes a negative term to the soil water alkalinity balance used to calculate the soil pH[4].

$$\text{Alk}_t = \text{Alk}_{t-1} + 2 \times (\text{Ca}_{\text{weath}} + \text{Mg}_{\text{weath}}) + \text{K}_{\text{weath}} + \text{Na}_{\text{weath}} - \Delta\text{Acidity}_N \quad (5)$$

This pH value is one component that is accounted for in the rate laws for mineral dissolution and therefore influences the net alkalinity produced at each depth within the soil profile, which contributes to CDR[4].

The initial alkalinity profile in each grid cell was determined from the starting soil pH and the partial pressure of CO_2 (p_{CO_2}) profile at steady state based on spin-up of the model with average long-term biomass production and soil organic matter decomposition that reflected the long-term land use history of a particular location. The alkalinity mass and flux balance for an adaptive time step accounted for alkalinity and acidity inputs from (1) mineral dissolution rates and secondary mineral precipitation (pedogenic carbonate), (2) biomass production and decomposition[64] and (3) biogeochemical N transformations. The soil pH profile was determined from an empirical soil pH buffering capacity[65] relating soil pH to the alkalinity at each depth. The soil p_{CO_2} depth profile of a grid cell was generated with the standard gas diffusion equation[66], scaled by monthly soil respiration from CLM5. At any particular location, the soil solution was in dynamic equilibrium with dissolved inorganic C species and the values of gas phase soil and atmospheric p_{CO_2}. The relative change induced by weathering will be the consumption of H^+ and the production of HCO_3^-.

Using this modelling framework (Extended Data Fig. 1), we analysed a baseline application rate of 40 t ha^{-1} yr^{-1} (equivalent to a <2-mm-thick layer of rock powder distributed on croplands) to UK croplands. Similar road transport of mass occurred in reverse during grain transport from field to market during UK harvest[67], indicating the appropriate capacity of rural transport networks to move basalt to the fields for ERW.

Gross CDR calculations. The gross CDR by ERW of crushed basalt applied to soils was calculated as the sum of two pathways: (1) the transfer of weathered base cations (Ca^{2+}, Mg^{2+}, Na^+ and K^+) from soil drainage waters to surface waters that are charge balanced by the formation of HCO_3^- ions and transported to the ocean (equation (6)), and (2) the formation of pedogenic carbonates (equation (7)).

Pathway 1 for calcium ions:

$$CaSiO_3 + 2CO_2 + 3H_2O \rightarrow Ca^{2+} + 2HCO_3^- + H_4SiO_4 \quad (6)$$

Pathway 2 for calcium carbonate formation:

$$Ca^{2+} + 2HCO_3^- \rightarrow CaCO_3 + CO_2 + H_2O \quad (7)$$

CDR, via pathway 1, potentially sequesters two moles of CO_2 from the atmosphere per mole of divalent cation. However, ocean carbonate chemistry reduces the efficiency of CO_2 removal to an extent, depending on ocean temperature, salinity and the dissolved CO_2 concentration of the surface ocean. We used annual ERW alkalinity flux time series (2020–2070) calculated with our 1D ERW model for S1 to S3 as inputs to GENIE (version 2.7.7)[68,69]. GENIE is an intermediate-complexity Earth system model with ocean biogeochemistry that allows computation of oceanic CDR via pathway 1. We used the same methodology as described previously[12] to simulate atmospheric CDR via the release of enhanced weathering alkalinity products into the ocean. The uncertainty for each scenario was determined by ensemble GENIE simulations with 84 different parameter sets that varied 28 parameters, each calibrated to simulate a reasonable pre-industrial and historical transient climate and carbon cycle[68–70]. CDR via pathway 2 occurred if dissolved inorganic carbon derived from atmospheric CO_2 precipitates as pedogenic carbonate, and sequestered 1 mol CO_2 per mole of Ca^{2+}.

Costs and carbon emissions of logistical operations. *Mining.* A breakdown of mining costs (in £ t^{-1}) of rock for the year 2010 and a representative granite mine with a daily 1,500 output and annual 375,000 output were obtained from a comprehensive analysis of UK aggregate mining[71]. Capital expenditure costs amounted to £24,395,636 over a 50-yr life cycle (£1.30 t^{-1} rock) whereas operating expenses (OPEX) amounted to £1,150,072 yr^{-1} (£3.07 t^{-1} rock) for a total £4.37 t^{-1} rock for the year 2010. To obtain cost projections over 2020–2070, the contributions of wages, diesel fuel and electricity consumption in OPEX (35.9%, 2.5% and 20.0% respectively) were normalized and projected for 2020–2070 using E3ME outputs of median wage, diesel prices and industrial electricity tariffs, respectively (Supplementary Information). Capital expenditure costs and the remaining OPEX (plant, buildings, equipment, tyres; in £ t^{-1} rock) remained constant over the period. Emissions of CO_2e t^{-1} rock extracted using diesel fuel and explosives were set at 4.29 kgCO_2e t^{-1} rock (ref. [71]). Emissions of CO_2e per unit of electricity consumed were obtained by combining electricity requirements per tonne of rock (1.48 kWh t^{-1} rock) and projected life cycle emissions (in kgCO_2e kWh^{-1}) from 2020 to 2070.

Grinding. Grinding breakdown costs were obtained from ref. [18]). Capital expenditure costs were set at £1.59 t^{-1} rock, while OPEX for plant, buildings and equipment were set at £0.97 t^{-1} rock. Diesel fuel and personnel costs (£0.08 t^{-1} rock and £0.85 t^{-1} rock for 2010) were projected to 2020–2070 using the methodology described above. We expressed electricity consumption per tonne of rock milled as a function of particle size, defined as p80[6]. To obtain electricity costs, we multiplied electricity consumption (in kWh t^{-1} rock milled) by E3ME projections of the unit cost of electricity (£ kWh^{-1}) and grinding emissions by multiplying electricity consumption by E3ME projections of electricity-production life cycle emissions (gCO_2e kWh^{-1}).

Spreading. Spreading costs were set at £8.3 t^{-1} rock for the year 2020 by averaging costs in the United Kingdom and United States[6]. Spreading costs were assigned equally to equipment, fuel/electricity and wages, with E3ME data used to provide cost projections to 2070 for the last two. A sigmoid function showing the transition to electric cars was obtained from E3ME, to which a 10 yr lag was added to signify delayed uptake by heavy agriculture vehicles (Supplementary Information). Spreading emissions were set at 0.003 kgCO_2 t^{-1} rock (ref. [18]). Our cost assessments assume that ERW practices are undertaken on farms as part of business-as-usual land-management practices. The pricing of external contracting of land management for rock dust application to soils is uncertain but could increase CDR prices per tCO_2 on the order of 10–15%.

Fertilizers. Projections of P fertilizer prices (2020–2070) for a global medium-resource scenario were obtained from ref. [72], showing an increase in global prices due to the depletion of phosphate reserves[72–74]. Even though K resources are also depleting, we kept K prices constant as alternative technologies and the opening of new mines in the Global South might alleviate the problem[75]. UK fertilizer prices for the year 2020 were used[31] as a baseline for our projections. Fertilizer savings were obtained as the product of release (in kg) of P and K by their unit price (£ kg^{-1}) over the time period 2020–2070. Life-cycle CO_2 emissions for P and K fertilizers were calculated as average values for different time horizons from the methodologies included in the Ecoinvent database[76] (Supplementary Information). Global markets for these products were selected for this analysis to include all that those fertilizers coming to the United Kingdom from any region of the world.

Energy requirements. Electricity supply characteristics for the United Kingdom were obtained from E3ME simulations (see the Transportation section). The annual electricity supply increases from 320 GWh yr^{-1} in 2020 to 637 GWh yr^{-1} in 2070, with life-cycle emissions dropping from 177.4 gCO_2 kWh^{-1} to −64.5 gCO_2 kWh^{-1}. The electricity mix profile shows an initial transition to onshore wind energy, followed by a marked uptake of solar and various CCS technologies.

The annual costs of ERW (in £ tCO_2^{-1}) CDR was obtained from equation (8) by summing the logistical costs for all locations (loc) (in £) that rock was applied according to each scenario for the particular year (y) and dividing by their total net CDR (in tCO_2) (equation (8)). Mining (Min) and spreading (Spread) costs are functions of the year, as the application rate was the same for all locations. Grinding (Grind) costs are a function of the year and p80. Transport (Transp) costs are function of the year and location, and consider the distance from the rock source. P and K release is a function of the year, p80 and location, as both particle size and location (climate) affect weathering rates and, subsequently, elemental release. All process costs are functions of the year due to time-varying wage, fuel, electricity and fertilizer costs.

$$\text{Costs}(y, \text{p80}) = \sum_{\text{Locations}} \frac{\text{Min}(y) + \text{Grind}(y,\text{p80}) + \text{Transp}(y,\text{loc}) + \text{Spread}(y) - \text{P}(y,\text{p80},\text{loc}) - \text{K}(y,\text{p80},\text{loc})}{\text{CO}_2\text{Gross Seq}(y,\text{p80},\text{loc}) - \text{CO}_2\text{Secondary Emissions}(y,\text{p80},\text{loc})} \quad (8)$$

Secondary emissions (in tCO_2) for each location were obtained by summing the emissions of each process (tCO_2 t^{-1} rock) in that year and multiplying by rock application (Rock) (in t rock) (equation (9))

$$\begin{aligned}&\text{CO}_2\text{Secondary Emissions}(y, \text{p80}, \text{loc})\\ &= [\text{Min}(y) + \text{Grind}(y, \text{p80}) + \text{Transp}(y, \text{loc})\\ &+ \text{Spread}(y) - \text{P}(y, \text{p80}, \text{loc}) - \text{K}(y, \text{p80}, \text{loc})]\\ &\times \text{Rock}(y, \text{loc})\end{aligned} \quad (9)$$

An initial run determined the order of the grid cells on the basis of their weathering potential. Rock was then applied, prioritizing grid cells with the highest potential, while the addition of rock in new areas each year was constrained by the annual rock availability of each scenario.

Transportation. Detailed transport analyses (based on UK road and rail networks) were undertaken to calculate distance costs and CO_2 emissions for the distribution of rock dust from source areas to croplands. We used the GLiM database for the UK distribution of basalt deposits[77] and the 2019 land cover map (Supplementary Information) to calculate transportation distances, cost (£ t^{-1} rock dust km^{-1}) and emissions ($tCO_2\,km^{-1}$) from potential local rock sources to cropland areas, together with UK road and rail transport networks[78]. Spatial analysis was undertaken with least-cost path algorithms from the ArcGIS software[79].

Wages and electricity/fuel prices and CO_2 emission factors were derived from E3ME's 1.5 °C energy scenario[2]. We started using typical fuel/electricity consumption values for both freight road (2.82 km l^{-1} and 3.07 kWh km^{-1})[71] and rail (98 km l^{-1})[76] to estimate the projected transport efficiency expressed in cost/emissions of a tonne of rock dust per kilometre (t km^{-1})[80–82]. Transport cost distribution per tonne-kilometre was derived using generic road and rail cost models that include wages, fuel, maintenance and depreciation[83,84]. The UK rail freight diesel-to-electricity decarbonization transition is already underway[85,86], and we used the continued projection for this transport mode. For road freight, the transport technology transition from the E3ME for electric vehicles was adopted, modified under the assumption that diesel ban policies and the availability of electric heavy goods vehicles for basalt transportation take place after 2030[87].

Energy and economic forecasts. UK energy–economic modelling (2020–2070)[88–90] was based on an updated version of the scenario described in ref. [17] that includes carbon pricing and has responses for the power sector (output and efficiency) consistent with government policy[91] (Supplementary Information). Total renewable energy sources over time were similar but with solar instead of 40 GW of offshore wind power. The simulations considered the phase-out of conventional vehicles by 2030, in line with government policy, and a consistent shift in aviation and freight towards biofuels, and electrified rail, as well as increased efficiency in buildings and the use of heat pumps. These simulations provide outputs for the United Kingdom for 2020 to 2070 of CO_2 emissions per unit energy, total energy mix and output, labour costs, electricity costs, fuel costs, and road and rail transport costs, which were inputs for calculating the costs of ERW CDR and secondary emissions during the grinding of rocks (Extended Data Fig. 2).

Data availability

Soil pH data were obtained from https://daac.ornl.gov/SOILS/guides/HWSD.html and http://www.ukso.org/. The high-resolution monthly fields of soil temperature and precipitation data were obtained from https://disc.gsfc.nasa.gov/datasets/FLDAS_NOAH01_C_GL_M_001/summary. Additional environmental and climate drivers were acquired through simulations of CLM5 available at https://github.com/ESCOMP/ctsm. The UK crop cover map was obtained from https://www.ceh.ac.uk/ukceh-land-cover-maps, annual time series of crop yields from https://www.fao.org/faostat/en/#data and UK fertilizer usage data from https://www.gov.uk/government/collections/fertiliser-usage. UK national border data were obtained from https://thematicmapping.org/downloads/world_borders.php. The GLiM v1.0 dataset used to identify rock sources is available at https://www.geo.uni-hamburg.de/en/geologie/forschung/aquatische-geochemie/glim.html. Datasets with 5 min resolution on global crop production and yield area to identify cropland are available at http://www.earthstat.org/harvested-area-yield-175-crops/. Datasets on road and rail vector data used for transport network analysis are available at http://www.diva-gis.org/gdata. Datasets on LCA impact factors used for K and P fertilizers are available within Ecoinvent 3.6 at https://ecoinvent.org/. Source data are provided with this paper.

Code availability

The weathering model was developed in MATLAB v.R2019a, and data processing was conducted in both MATLAB v.R2019a and Python v.3.7. MATLAB and Python codes developed for this study belong to the Leverhulme Centre for Climate Change Mitigation. These codes, and the modified codes in CLM5 developed in this study, are available from the corresponding author upon reasonable request.

References

51. Palandri, J. L. & Kharaka, Y. K. *A Compilation of Rate Parameters of Water-Mineral Interaction Kinetics for Application to Geochemical Modelling* (USGS, 2004).
52. Lawrence, D. M. et al. The Community Land Model version 5: description of new features, benchmarking, and impact of forcing uncertainty. *Adv. Model. Earth Sys.* **11**, 4245–4287 (2019).
53. Lawrence, D. M. et al. *Technical Description of Version 5.0 of the Community Land Model (CLM)* (National Center for Atmospheric Research, 2020).
54. Wieder, W. R. et al. Beyond static benchmarking: using experimental manipulations to evaluate land model assumptions. *Glob. Biogeochem. Cycles* **33**, 1289–1309 (2019).
55. Lombardozzi, D. L. et al. Simulating agriculture in the Community Land Model Version 5. *J. Geophys. Res. Biogeosci.* **125**, e2019JG005529 (2020).
56. Lawrence, D. M. et al. The Land Use Model Intercomparison Project (LUMIP) contribution to CMIP6: rationale and experimental design. *Geosci. Mod. Dev.* **9**, 2973–2998 (2016).
57. Thomson, A. et al. *Quantifying the Impact of Future Land Use Scenarios to 2050 and Beyond* (Rothamsted Research, 2018).
58. *British Survey of Fertiliser Practice: Fertiliser Use on Farm for the 2018 Crop Year* (DEFRA, 2019); https://assets.publishing.service.gov.uk/government/uploads/system/uploads/attachment_data/file/806642/fertiliseruse-statsnotice2018-06jun19.pdf
59. Fung, K. M., Val Martin, M. & Tai, A. P. K. Modeling the interinfluence of fertilizer-induced NH_3 emission, nitrogen deposition, and aerosol radiative effects using modified CESM2. *Biogeosciences* **19**, 1635–1655 (2022).
60. IPCC *IPCC Guidelines for National Greenhouse Gas Inventories Prepared by the National Greenhouse Gas Inventories Programme* (eds Eggleston, H. S. et al.) (IGES, 2006).
61. *Refinement to the 2006 IPCC Guidelines for National Greenhouse Gas Inventories* (eds Calvo Buendia, E. et al.) (IPCC, 2019).
62. Hartmann, J. & Kempe, S. What is the maximum potential for CO_2 sequestration by "stimulated" weathering on the global scale? *Naturwissenschaften* **95**, 1159–1164 (2008).
63. Taylor, L. L. et al. Increased carbon capture by a silicate-treated forested watershed affected by acid deposition. *Biogeosciences* **18**, 169–199 (2021).
64. Banwart, S. A., Berg, A. & Beerling, D. J. Process-based modelling of silicate mineral weathering responses to increasing atmospheric CO_2 and climate change. *Glob. Biogeochem. Cycles* **23**, GB4013 (2009).
65. Nelson, P. N. & Su, N. Soil pH buffering capacity: a descriptive function and its application to some acidic tropical soils. *Aust. J. Soil Sci.* **48**, 201–207 (2010).
66. Cerling, T. Carbon dioxide in the atmosphere: evidence from Cenozoic and Mesozoic paleosols. *Am. J. Sci.* **291**, 377–400 (1991).
67. Holland, J. E. et al. Yield responses of arable crops to liming – an evaluation of relationships between yields and soil pH from a long-term liming experiment. *Eur. J. Agron.* **105**, 176–188 (2019).
68. Holden, P. B., Edwards, N. R., Gerten, D. & Schaphoff, S. A model-based constraint on CO_2 fertilisation. *Biogeosciences* **10**, 339–355 (2013).
69. Holden, P. B. et al. Controls on the spatial distribution of oceanic $\delta^{13}C$ DIC. *Biogeosciences* **10**, 1815–1833 (2013).
70. Foley, A. M. et al. Climate model emulation in an integrated assessment framework: a case study on mitigation policies in the electricity sector. *Earth Syst. Dynam.* **7**, 119–132 (2016).
71. Brown, T. J. et al. *Underground Mining of Aggregates Main Report* ASRP Project No. 7 (British Geological Survey, 2010).
72. Van Vuuren, D. P., Bouwman, A. F. & Beusen, A. H. W. Phosphorus demand for the 1970-2100 period: a scenario analysis of resource depletion. *Glob. Environ. Change* **20**, 428–439 (2010).
73. Alewell, C. et al. Global phosphorus shortage will be aggravated by soil erosion. *Nat. Commun.* **11**, 4546 (2020).
74. Gilbert, N. The disappearing nutrient. *Nature* **461**, 716–718 (2009).
75. Ciceri, D., Manning, D. A. C. & Allanore, A. Historical and technical developments of potassium resources. *Sci. Total Environ.* **502**, 590–601 (2015).
76. Wernet, G. et al. The ecoinvent database version 3 (part I): overview and methodology. *Int. J. Life Cycle Assess.* **21**, 1218–1230 (2016).
77. Hartmann, J. & Moosdorf, N. The new global lithological map database GLiM: a representation of rock properties at the Earth surface. *Geochem. Geophys. Geosyst.* **13**, Q12004 (2012).
78. *Strategy, Road and Rail Vector Data* (Ordnance Survey, 2016).
79. Maguire, D. J. in *Encyclopedia of GIS* (eds Shekhar, S. & Xiong, H.) 25–31 (Springer, 2008).
80. Wilkins, J. *Transport Statistics Great Britain 2017* 79 (Department for Transport, 2017).
81. *The Future of Rail: Opportunities for Energy and the Environment* (International Energy Agency, 2019).
82. Delgado, O., Rodríguez, F. & Moncrieff, R. *Fuel Efficiency Technology in European Heavy-Duty Vehicles: Baseline and Potential for the 2020–2030 Time Frame* (International Council of Clean Transportation, 2017).
83. SMMT *Truck Specification for Best Operational Efficiency Guide* (Department for Transport, 2010).
84. *Analysis of Road and Rail Costs Between Coal Mines and Power Stations* (MDS Transmodal Limited, 2012).
85. *Rail Freight Market Share: Freight Rail Usage and Performance 2020-21 Quarter 3* 10 (Office of Rail and Road, UK National Statistics, 2021).
86. Beeson, R. *The Rail Central Rail Freight Interchange* Appendix 21.2 (National Infrastructure Planning, 2018).
87. Liimatainen, H., van Vliet, O. & Aplyn, D. The potential of electric trucks—an international commodity-level analysis. *Appl. Energy* **236**, 804–814 (2019).
88. Mercure, J. F. et al. Macroeconomic impact of stranded fossil fuel assets. *Nat. Clim. Change* **8**, 588–593 (2018).
89. *E3ME Manual: Version 6.1* (Cambridge Econometrics, 2019); https://www.e3me.com/what/e3me/
90. Mercure, J.-F. et al. Environmental impact assessment for climate change policy with the simulation-based integrated assessment model E3ME-FTT-GENIE'. *Energy Strat. Rev.* **20**, 195–208 (2018).

91. *The Energy White Paper: Powering Our Net Zero Future* (HM Government, 2020).

Acknowledgements

We thank C. Le Quéré, A. Collins, R. Freckleton, J. Leake and J. Scurlock for comments on an earlier draft. We gratefully acknowledge funding of this research under a Leverhulme Research Centre Award (RC-2015–029; D.J.B.) from the Leverhulme Trust. D.J.B. and P.R. acknowledge UKRI funding under the UK Greenhouse Gas Removal Programme (BB/V011359/1, D.J.B.; NE/P019943/1, NE/P019730/1, P.R.). M.V.M. acknowledges funding from the UKRI Future Leaders Fellowship Programme (MR/T019867/1). We to acknowledge high-performance computing support from Cheyenne (doi: 10.5065/D6RX99HX) provided by NCAR's Computational and Information Systems Laboratory, sponsored by the National Science Foundation. We acknowledge the World Climate Research Programme's Working Group on Coupled Modelling responsible for CMIP and thank the climate modelling groups for producing and making available their model output. For CMIP, the US Department of Energy's Program for Climate Model Diagnosis and Intercomparison provides coordinating support and led development of software infrastructure in partnership with the Global Organization for Earth System Science Portals.

Author contributions

D.J.B., E.P.K., M.V.M., M.R.L., P.R. and S.A.B. designed the study. E.P.K., M.V.M and M.R.L. undertook model development, simulations and coding, with input from L.L.T., S.A.B. and D.J.B. E.P.K. undertook data analysis and synthesis. R.M.E. undertook the UK transport analyses with input from L.K. P.R. developed the silicate supply scenarios, A.L.L. undertook the X-ray diffraction analyses of UK basalts and N.F.P. wrote sections on public perception. N.V. and P.B.H. undertook the GENIE analyses. J.-F.M., H.P., P.V.V., N.R.E. and P.B.H. provided analyses and data on UK national economics, energy production and CO_2 emissions. L.L.T. led the drafting of the Supplementary Information. D.J.B. and S.A.B. wrote the manuscript with input from co-authors.

Competing interests

The authors declare no competing interests.

Additional information

Extended data is available for this paper at https://doi.org/10.1038/s41561-022-00925-2.

Supplementary information The online version contains supplementary material available at https://doi.org/10.1038/s41561-022-00925-2.

Correspondence and requests for materials should be addressed to David J. Beerling.

Peer review information *Nature Geoscience* thanks Thorben Amann and Ward Smith for their contribution to the peer review of this work. Primary Handling Editors: Kyle Frischkorn and Tom Richardson, in collaboration with the *Nature Geoscience* team.

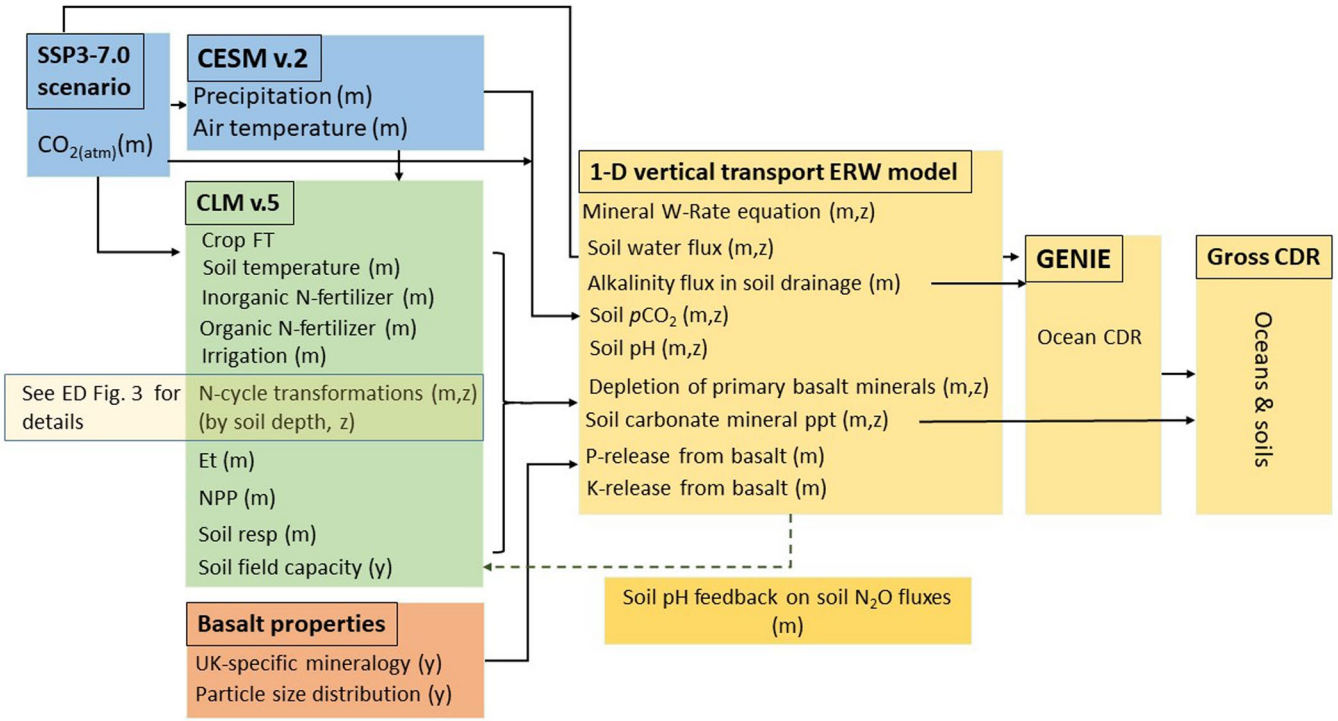

Extended Data Fig. 1 | Coupled climate-C-N cycle modelling framework. Schematic overview of coupled climate-carbon-nitrogen modelling strategy for simulating carbon dioxide removal (CDR) with enhanced rock weathering (ERW). CESM, the Community Earth System Model v.2; CLM5, the Community Land Model v.5. Abbreviations. m = monthly time step, y = yearly time step, z = depth.

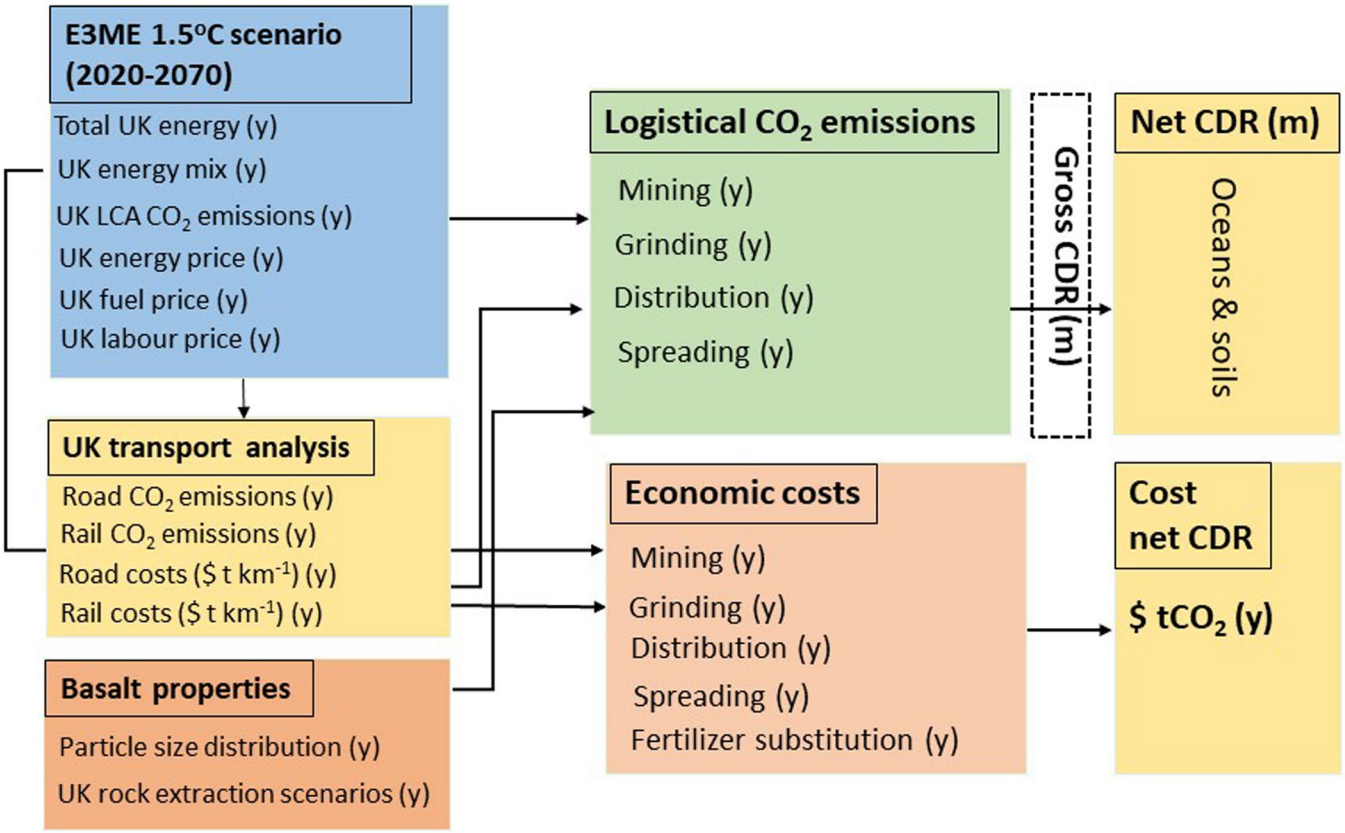

Extended Data Fig. 2 | Logistical CO_2 emissions and costs of ERW modelling framework. Annual (y) energy, economic and transport outputs from E3ME, together with road and rail network analyses, are used to calculate CO_2 emissions from ERW logistical operations and costs. The resulting CO_2 emissions are subtracted from gross CDR to estimate net CDR and costs of net CDR.

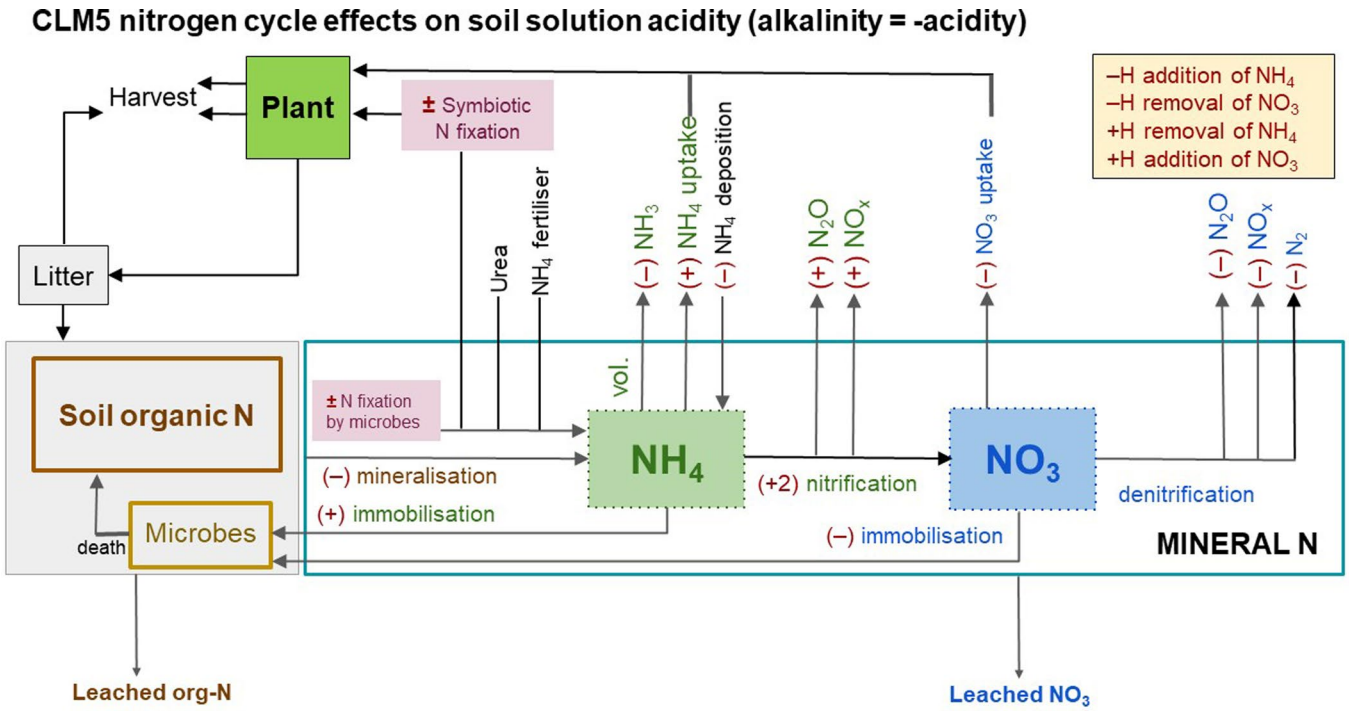

Extended Data Fig. 3 | Representation of nitrogen cycle transformations on soil acidity. Nitrogen cycle transformations represented by the CLM5 land surface model coupled to our soil profile ERW modelling. Indicated is the proton gain or loss associated with each reaction.

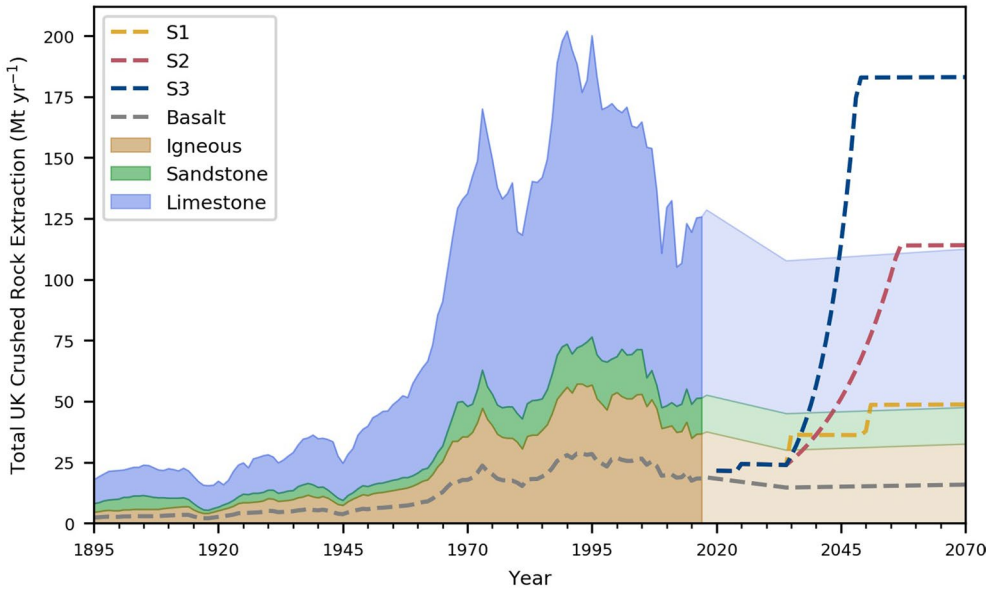

Extended Data Fig. 4 | Resource extraction scenarios compared with the historical record. Resource extraction scenarios compared with the historical record. Estimated basalt rock extraction (grey line) and three basalt extraction scenarios (S1-low): 'maintain 2018 number of mines (+32 Mt yr^{-1})', (S2-medium): 'total rock extraction equivalent to previous 1990 maximum rate (+97 Mt yr^{-1})', and S3-high 'total capacity increase equivalent to 1945 to 1990 (166 Mt yr^{-1})') to provide material for ERW simulations reported here. S2 essentially diverts the 100 Mt yr^{-1} drop in production since 1990 into basalt extraction for CDR, and S3 adopts a rock extraction rate (+166 Mt yr^{-1}) comparable to that reported for 1945–1990 (~180 Mt yr^{-1}). These historical constraints underpin the plausibility of S2 and S3.

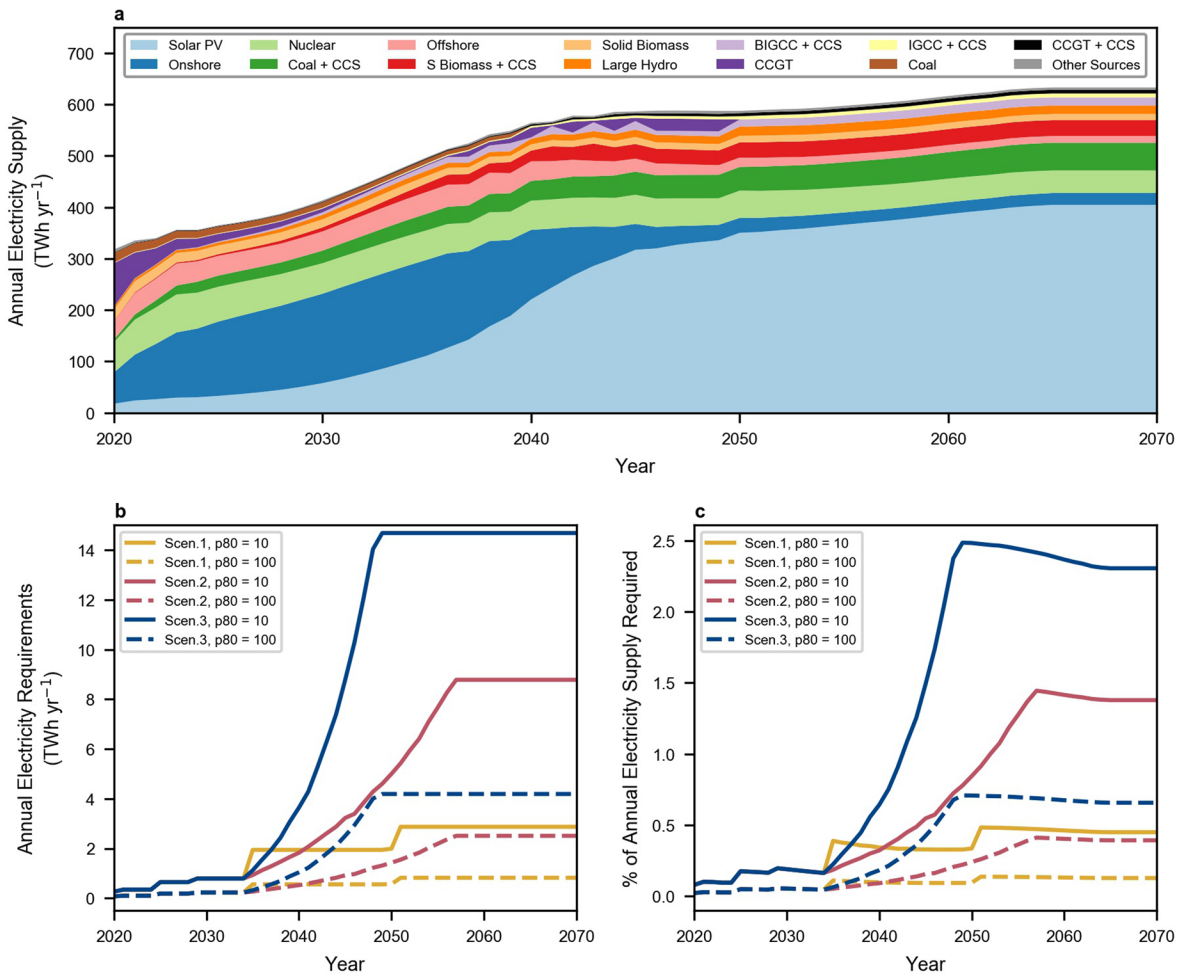

Extended Data Fig. 5 | UK energy production and demand for rock grinding. UK energy production and demand for rock grinding. (a) Energy mix and total annual UK supply modelled by E3ME, (b) absolute energy requirement for rock grinding for three scenarios and (c) percentage of annual UK energy required for rock grinding for the three scenarios.

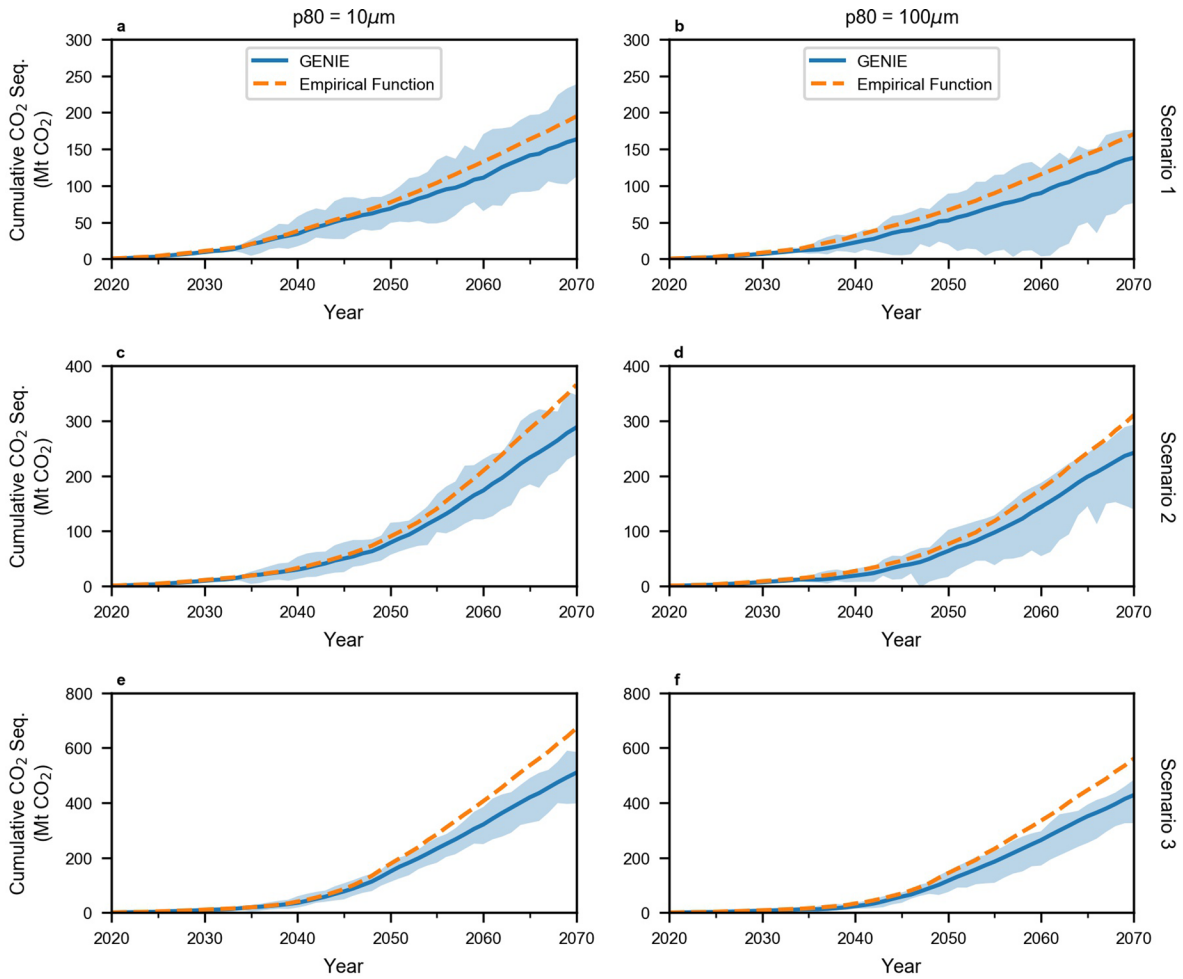

Extended Data Fig. 6 | Uncertainty in ocean CDR with ERW. Uncertainty in ocean CDR with ERW. Results show ocean CDR simulated by the intermediate complexity Earth System Model, Genie (blue line), and an empirical function accounting CO_2, ocean temperature and salinity[6] (red dashed line). Panels display results for simulations of scenario 1 for rock grain (a) p80 = 10 μm and (b) p80 =100 μm, scenario 2 for rock grain (c) p80 = 10 μm and (d) p80 =100 μm, and scenario 3 for rock gain (e) p80 = 10 μm and (f) p80 =100 μm. Genie uncertainties represent 90% confidence limits based on ensemble simulations with 84 different parameter sets. The difference the result of Earth system feedbacks in Genie whereby atmospheric CO_2 lowered by ERW causes oceanic outgassing, and sediment $CaCO_3$ uptake reduces alkalinity. Simulations use annual alkalinity fluxes generated by the 1-D soil profile weathering with three UK basalts.

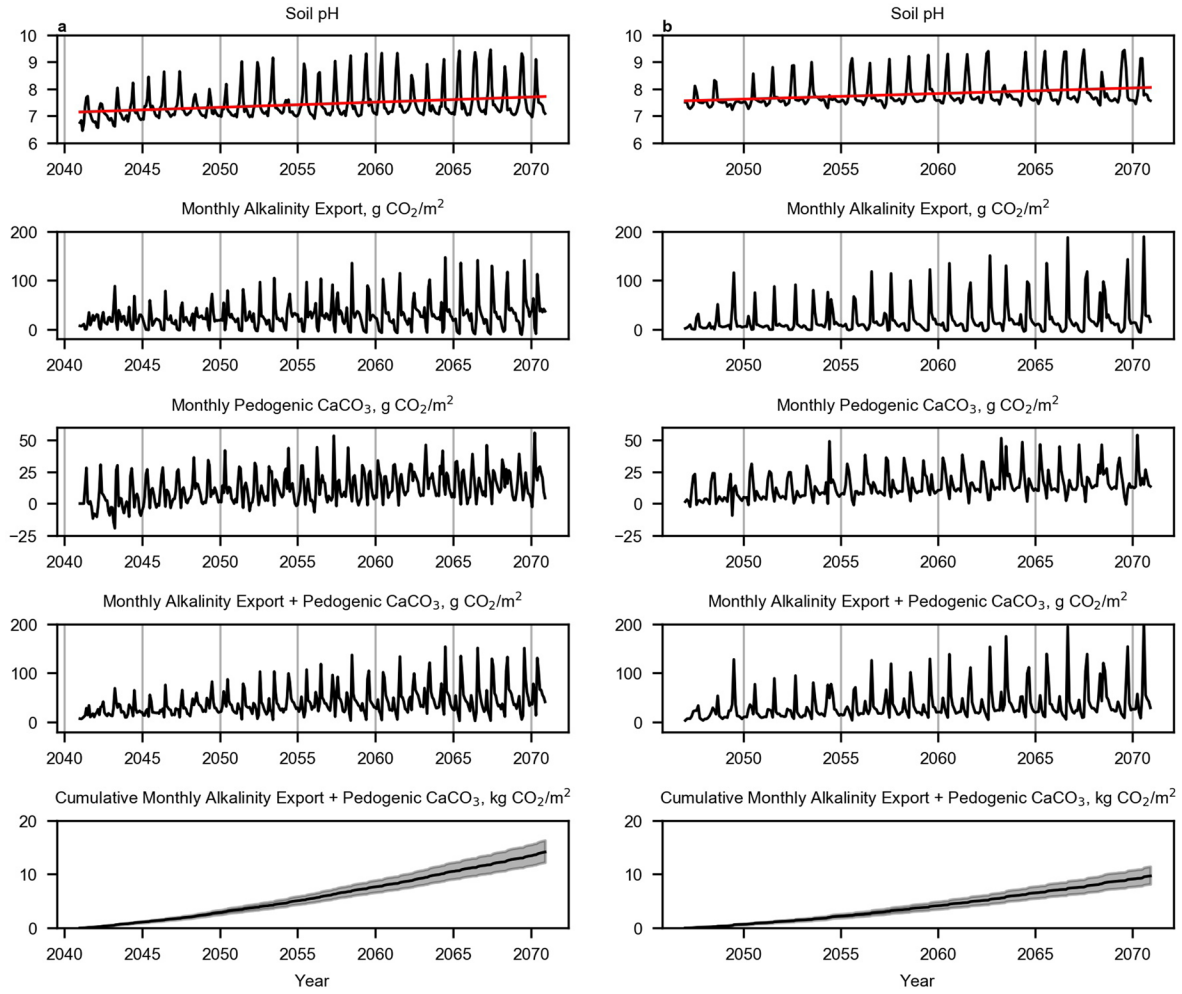

Extended Data Fig. 7 | Seasonal variations in soil CDR pathway time-series. Seasonal variations in soil CDR pathway time-series. Illustrative time-series of model dynamics of the two CDR pathways (soil export of alkalinity and formation/dissolution of carbonates) and pH. Simulations were undertaken for Cragmill basalt mineralogy with p80 particle diameter of 100 μm. Left-hand site: winter barley (midlands), right hand site: winter wheat (south east).

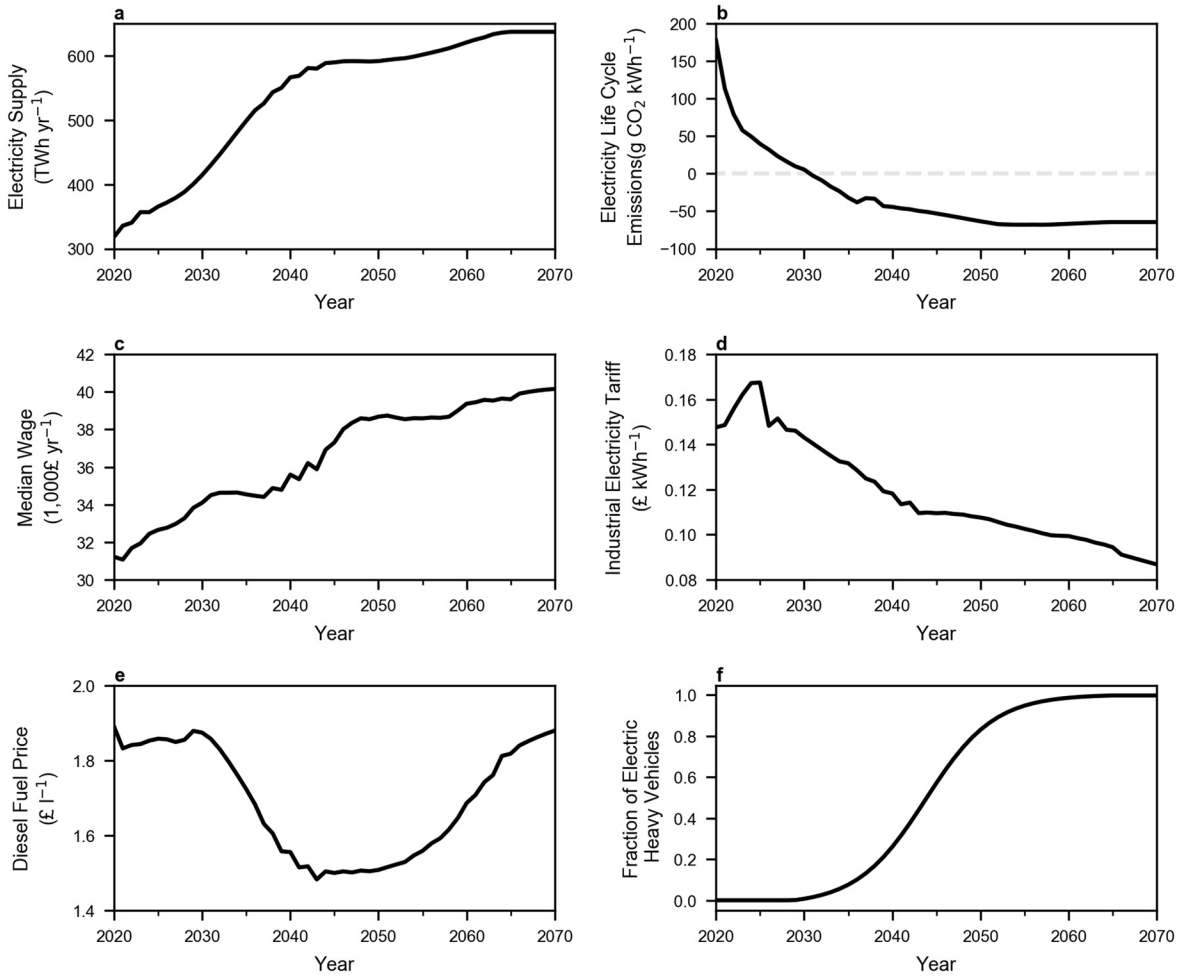

Extended Data Fig. 8 | Simulated UK energy and economic drivers (2020–2070). Simulated UK energy and economic drivers (2020–2070). (**a**) modelled evolution of UK energy supply and mix consistent with specific policies in the 1.5 °C scenario, (**b**) life cycle CO_2 emissions of energy production, (**c**) median wage rates, (**d**) industrial electricity tariff with the rapid transition to renewable generation, (**e**) diesel fuel prices and (**f**) modelled transitional uptake of electric heavy goods transportation.

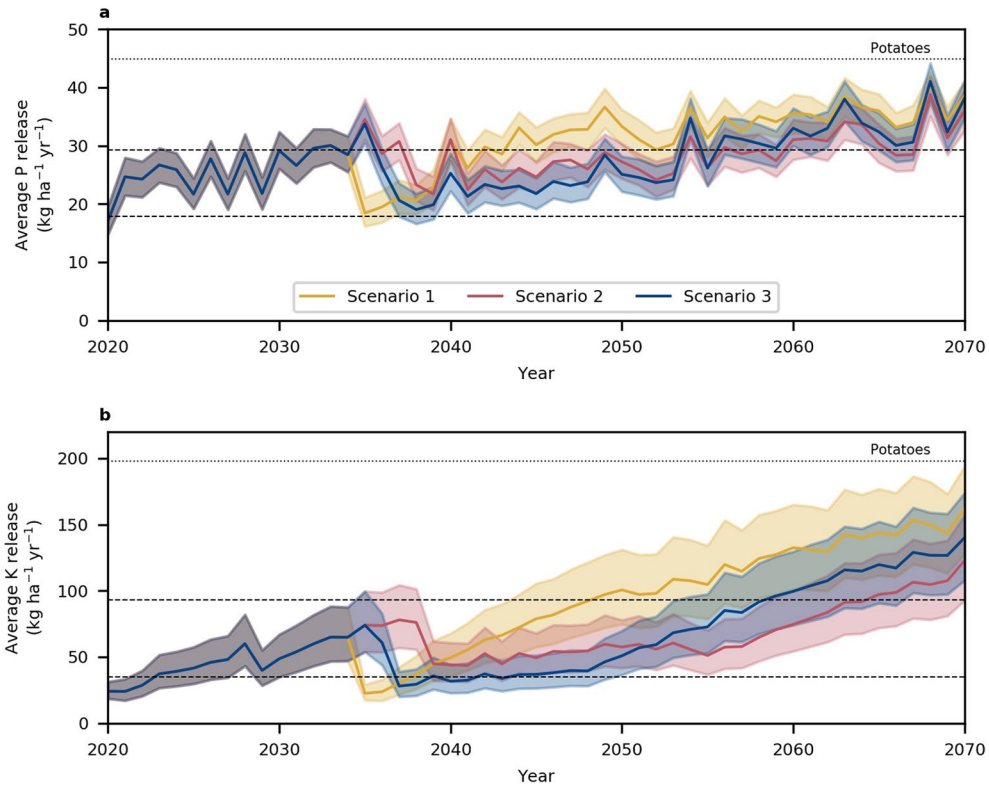

Extended Data Fig. 9 | Potential mineral nutrient release rates from ERW. Modelled mineral nutrient release rates from ERW. P- and K-mass transfer from rocks to soil are the mean of simulations for three UK-specific basalts and two p80 values (10 μm and 100 μm diameter). Shaded envelopes show the 95% confidence limits. Dashed lines indicate upper and lower range of major UK tillage crops. Scenario 1 has fewest grid cells but ERW deployment starts early and average release rate increases with repeated rock dust applications. Scenarios 2 and 3 add more grid cells with initial lower release rates causing the average release rate to remain constant. Elements are likely to be retained in the soil column on ion exchange clays (K), and sorbed on secondary minerals (P), for example iron oxides.